Review

Update on the Applications of Radiomics in Diagnosis, Staging, and Recurrence of Intrahepatic Cholangiocarcinoma

Maria Chiara Brunese [1], Maria Rita Fantozzi [2], Roberta Fusco [3,*], Federica De Muzio [1], Michela Gabelloni [4], Ginevra Danti [5,6], Alessandra Borgheresi [7,8], Pierpaolo Palumbo [9], Federico Bruno [9], Nicoletta Gandolfo [10], Andrea Giovagnoni [7,8], Vittorio Miele [5,6], Antonio Barile [11] and Vincenza Granata [12]

1   Department of Medicine and Health Sciences "V. Tiberio", University of Molise, 86100 Campobasso, Italy
2   Clinical Pharmacology Unit, A. Cardarelli Hospital, 86100 Campobasso, Italy
3   Medical Oncology Division, Igea SpA, 80013 Naples, Italy
4   Nuclear Medicine Unit, Department of Translational Research, University of Pisa, 56126 Pisa, Italy
5   Italian Society of Medical and Interventional Radiology (SIRM), SIRM Foundation, Via della Signora 2, 20122 Milan, Italy
6   Department of Emergency Radiology, Careggi University Hospital, Largo Brambilla 3, 50134 Florence, Italy
7   Department of Radiology, University Hospital "Azienda Ospedaliera Universitaria delle Marche", 60121 Ancona, Italy
8   Department of Clinical, Special and Dental Sciences, Università Politecnica delle Marche, 60121 Ancona, Italy
9   Department of Diagnostic Imaging, Area of Cardiovascular and Interventional Imaging, Abruzzo Health Unit 1, 67100 L'Aquila, Italy
10 Diagnostic Imaging Department, Villa Scassi Hospital-ASL 3, 16149 Genoa, Italy
11 Department of Biotechnological and Applied Clinical Sciences, University of L'Aquila, 67100 L'Aquila, Italy
12 Division of Radiology, Istituto Nazionale Tumori IRCCS Fondazione Pascale—IRCCS di Napoli, 80131 Naples, Italy
*   Correspondence: r.fusco@igeamedical.com

Abstract: Background: This paper offers an assessment of radiomics tools in the evaluation of intrahepatic cholangiocarcinoma. Methods: The PubMed database was searched for papers published in the English language no earlier than October 2022. Results: We found 236 studies, and 37 satisfied our research criteria. Several studies addressed multidisciplinary topics, especially diagnosis, prognosis, response to therapy, and prediction of staging (TNM) or pathomorphological patterns. In this review, we have covered diagnostic tools developed through machine learning, deep learning, and neural network for the recurrence and prediction of biological characteristics. The majority of the studies were retrospective. Conclusions: It is possible to conclude that many performing models have been developed to make differential diagnosis easier for radiologists to predict recurrence and genomic patterns. However, all the studies were retrospective, lacking further external validation in prospective and multicentric cohorts. Furthermore, the radiomics models and the expression of results should be standardized and automatized to be applicable in clinical practice.

Keywords: radiomics; diagnosis; staging; recurrence; intrahepatic cholangiocarcinoma

1. Introduction

Cholangiocarcinoma (CCA) is the liver's second most common primary malignancy [1,2]. Due to the increasing incidence of CCA, several studies have focused on improving the diagnosis, prognosis, and treatment of patients [3]. CCA diagnosis is routinely achieved through serum markers (CA 19-9, CEA) and radiologic imaging, but in atypical cases, differential diagnosis can be still challenging, so biopsy remains the only tool for definitive diagnosis [4].

Intrahepatic cholangiocarcinoma (ICC) is the most common type of cholangiocarcinoma, and according to pathological classification, it is categorized as mass forming,

periductal infiltrating, or intraductal growing [5]. Among the different subtypes, the mass-forming subtype represents 78% of cases [5,6]. Its main morphological pattern is abundant stromal fibrosis, which also influences its radiological imaging behavior [7,8].

Despite the challenging nature of this task, conducting a differential diagnosis between ICC and other liver lesions, especially concerning HCC and combined hepatocellular cholangiocarcinoma (Figure 1), is mandatory to conduct appropriate treatment planning [9,10]. To help radiologists and clinicians, several authors have proposed radiomics models to better define tumor characteristics and disease progression [11,12].
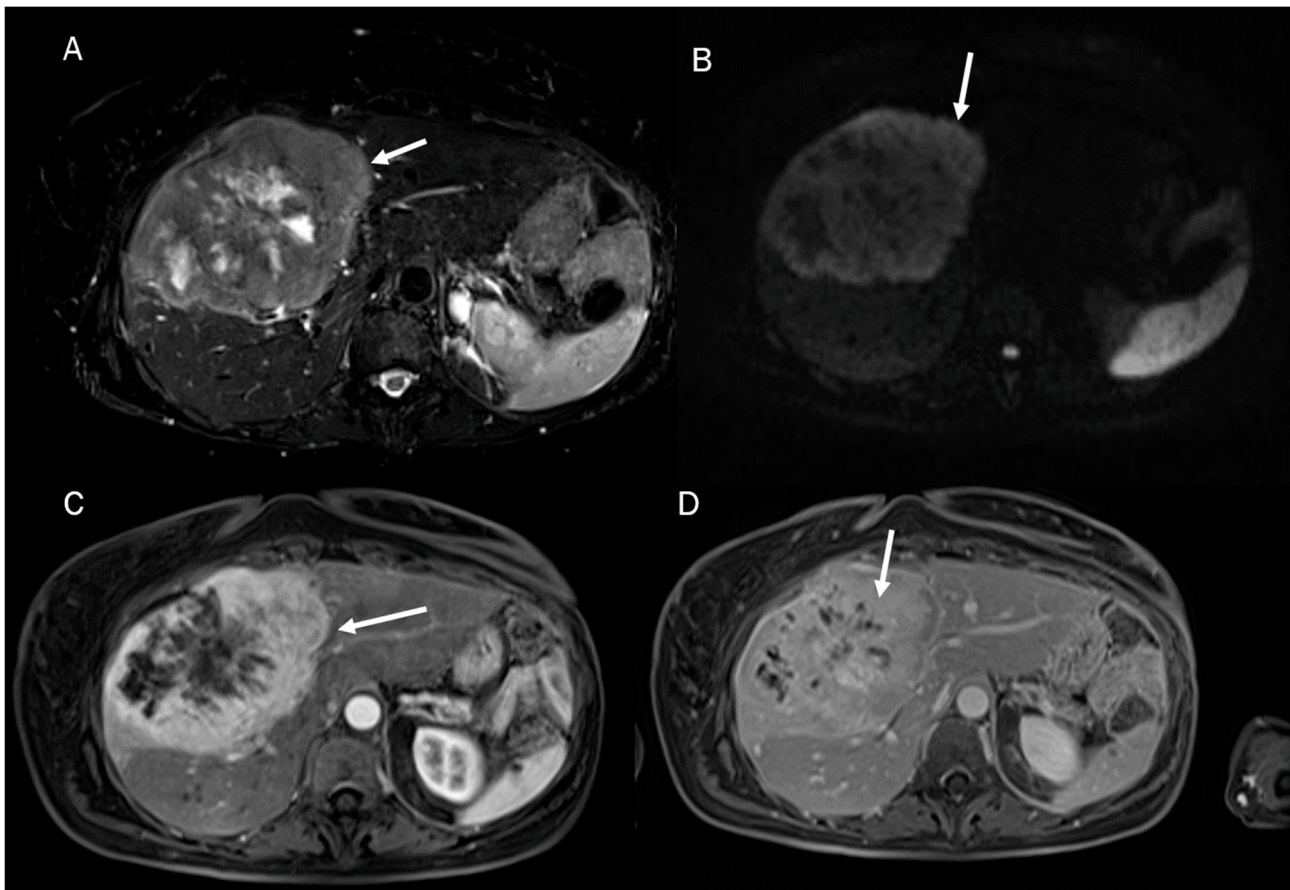
Figure 1. Combined hepatocellular cholangiocarcinoma MRI assessment: the lesion (arrow) shown in T2-W sequence (**A**); targetoid appearance, with restricted diffusion in b800 s/mm^2 (**B**); and progressive contrast enhancement during contrast study (arterial phase (**C**) and portal phase (**D**)).

Radiomics belongs to the wider field of artificial intelligence (AI). The most common AI tools are based on machine learning and statistical analysis, while deep learning and neural network represent the most frequent subset [13,14]. The most relevant drawback of machine-learning (ML) AI is the need for a considerable number of data to train the program, so another AI pathway, known as formal methods (FMs), is slowly becoming a reliable tool. This pathway does not need a large sample of images because it is not based on a training set. FMs are defined based on pre-defined rules built on clinical features turned into a numeric and informatic code [15–18]. The machine-learning approach is the most commonly used. It is capable of learning a large amount of information, so it is gaining even more diffusion in many fields beyond radiology, like nuclear medicine and clinical fields [19,20]. In order to train the most reliable radiomics model, ML was applied to the ultrasound (US) Computed Tomography (CT) or Magnetic Resonance Imaging (MRI) gold-standard protocols already in use for diagnosis, staging, or follow-up in current clinical practice [20–23]. Radiomics has also demonstrated dependable results differentiating

benign from malignant pathologies in many fields whenever treatment strategies could have been radically different [24,25].

Nowadays, radiomics applications are primarily common in oncology concerning neurological, breast, pulmonary, abdominal, and pelvic diseases [26–28]. However, the COVID-19 pandemic asked for the earliest diagnosis [29,30]. In this emergency context, radiomics had the chance to demonstrate its efficacy and feasibility; it improved diagnostic accuracy, answering a wide number of clinical questions, and it did so outside of referral centers due to the limitations on mobility for sanitary reasons [31–34]. At the same time, its limits became evident per a small number of studies focused on its explainability, while in clinical practice, many tools required a long work time and the necessity of standardization of the analysis [35–38]. In the large field of diagnosis, radiomics has been first developed to classify different lesions in order to avoid further more invasive exams [39,40]. Subsequent applications of radiomics have been found in predicting tumor grade and helping radiologists detect challenging precancerous syndromes [41–46]. The latest fashion in AI application is represented by the role of radiomics in the prediction of response to surgical or medical treatment in cancer patients [47–51]. In this way, radiomics can be used to speculate as to the risk category classification of patients and to predict patient overall survival and risk of complication [52–60].

Hepatobiliary and pancreatic cancers have been deeply investigated through AI methods [61]. Authors have aimed to recognize primitive and metastatic lesions or to distinguish benign lesions from malignant ones when the limits of conventional imaging techniques did not allow a proper differential diagnosis [62,63]. The most frequent application of radiomics has involved CT scan; however, growing interest has been shown regarding integrated imaging [64–67].

As depicted above, ICC represents a natural field of interest of radiomics tools due to its ability to exhibit atypical behavior that makes, in some cases, the diagnosis and the subsequent treatment strategy very challenging [4–6]. The aim of this review is to report the results of several studies and the real application of radiomics in clinical practice in the large field of diagnosis. The included studies address the following main topics: the prediction of recurrence, the assessment of lymph node status, and the prediction of tumor mutation.

2. Methods

We searched the PubMed database (US National Library of Medicine, http://www.ncbi.nlm.nih.gov/PubMed accessed on 15 October 2022) using the subsequent keywords: (((artificial intelligence) OR (radiomics) OR (convolutional neural networks) OR (machine learning) OR (radiomic) OR (deep learning) OR (ultrasomics)) AND ((cholangiocarcinoma) OR (cholangiocellular carcinoma) OR (biliary tumor) OR (Klatskin) OR (hepatocellular cholangiocarcinoma) OR (Combined hepatocellular cholangiocarcinoma)) AND ("English" [Language])).

Papers had to have been published no earlier than October 2022. Articles were first chosen based on title and abstract, but a review of the available full text was necessary to definitely include the article. Clinical studies (retrospective analysis, case series, prospective cohort study) were reviewed. Case reports, reviews, comments, or letters to editors were excluded.

3. Results

We recognized 238 pertinent papers. We narrowed down to 89 papers based on a review of titles and abstracts. Then we narrowed further to 61 full-text articles concerning the improvement of diagnosis and treatment strategy.

Articles first excluded for title and abstract were reviews or case reports, or they did not address ICC. Full-text articles excluded did not clearly explain methods and results about diagnosis, recurrence, and staging of ICC.

A total of 34 clinical studies, concerning diagnosis, recurrence, and staging, were assessed in this narrative review. The reference flow is summarized in the study flow diagram (Figure 2).
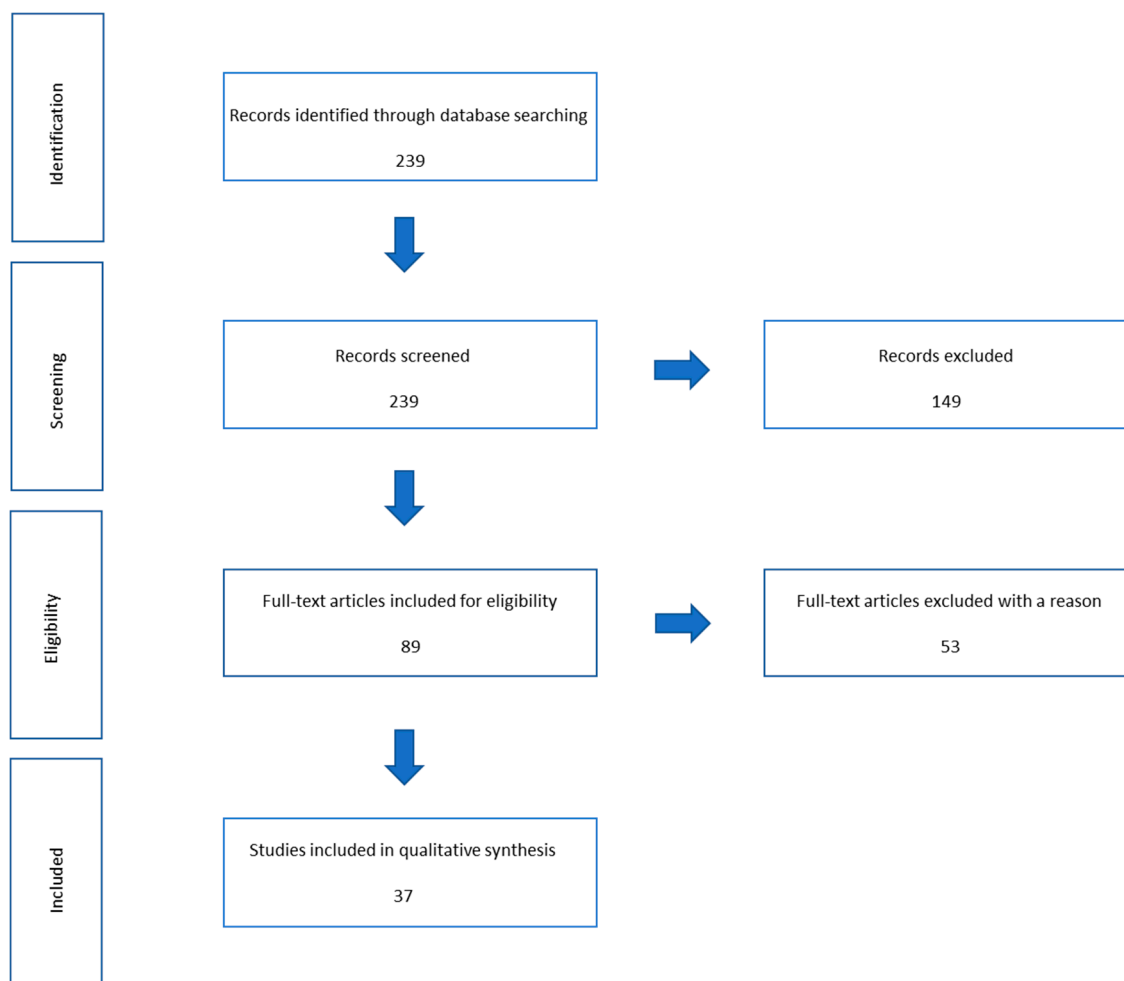

Figure 2. Flowchart of included and excluded studies.

3.1. Ultrasound

Ultrasound is an inexpensive, non-invasive imaging tool that is not based on X-ray sources [68–72]. Its plasticity allows operators to best manage uncompliant patients [73–76]. To overcome several US limits, and to achieve a non-invasive diagnosis, in the last decades, a new technique has been developed mostly based on contrast-enhanced ultrasound (CEUS), or even on shear-wave elastography combined with a CEUS algorithm [77].

CEUS is now used to study large vessel flows and the microcirculation and US behavior of oncological lesions, which might be very helpful for differential diagnosis between benign and malignant tumors [78]. Liver lesions contrast study includes: (1) the arterial phase, which starts at 10–20 s and ends 30–45 s after contrast injection; (2) the portal venous phase, which lasts from 30–45 s to 2 min after contrast agent injection; and (3) the delayed phase, which lasts from 4 to 6 min after the contrast injection [79].

In US studies, mass-forming ICC occurs as a large non-encapsulated mass with lobulated or variable shape. It can also be associated with liver capsule retraction and dilated peripheral bile ducts [80]. With respect to its pathomorphological characteristics (necrosis, fibrosis, and tumor growth), ICC can show a heterogeneous basal-US echogenicity pattern [81]. During CEUS assessment, ICC could show hyperenhancement during the arterial phase (Figure 3) with washout. According to several authors, ICC washout at its earliest stage is comparable to HCC, and this finding should guide a correct diagnosis [82–84].
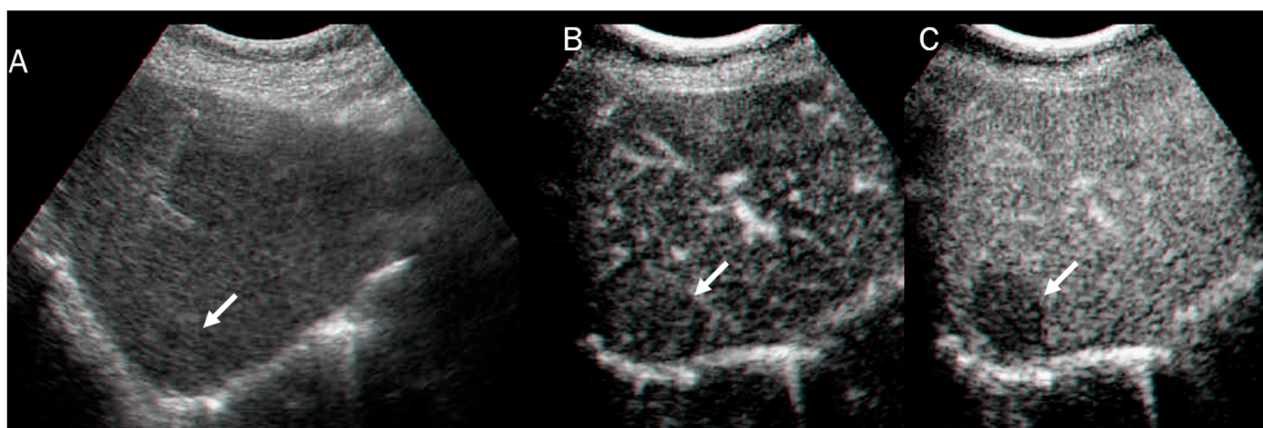
Figure 3. US and CEUS assessment of ICC: On US (**A**), the lesion (arrow) shows iso-hypoechoic pattern compared to hepatic parenchymal. During arterial phase (**B**), the lesion shows arterial hyperenhancement (arrow), with washout (arrow) in portal phase (**C**).

As shown in international guidelines, the differential diagnosis between HCC and ICC can be challenging, especially in non-cirrhotic patients, where the typical radiological pictures of mass-forming ICC might be very similar to pictures of HCC enhancement pattern, requiring liver biopsy to achieve the correct diagnosis [85]. CEUS achieved a reliable sensitivity in differentiating ICC from HCC of 0.92 with a pooled specificity of 0.87 [86,87]. Considering that the diagnostic performance of CEUS is very changeable as the diagnostic technique is operator-dependent, ultrasomics surely could make the US exams more repeatable and reliable, standardizing the technique; in fact, in the comparison studies between radiologists and ultrasomics model performance, the latter achieved a better sensitivity and global accuracy [87]. Ultrasomics has been proven to be useful in the early diagnosis, preoperative grading prediction, therapeutic efficacy evaluation, and prognosis evaluation of several tumors [88–93].

Regarding the differential diagnosis of liver lesions, ultrasomics-based studies achieved a good accuracy in the validation or test set [89,90]. In a study by Peng et al., patients were classified into 3 groups: 89 ICC, 531 HCC, and 48 combined hepatocellular cholangiocarcinoma (cHCC-ICC). The overall performance of the radiomics model in identifying different histopathological subtypes was moderate, with AUC values of 0.854 (training cohort) and 0.775 (test cohort) in the HCC vs. non-HCC model and 0.920 (training cohort) and 0.728 (test cohort) in the ICC vs. cHCC-ICC radiomics model [89]. Ren et al. assessed two subgroups: HCC and non-HCC. The combined (clinical + radiomics) model achieved the highest accuracy in the external validation set, with an AUC of 0.874, a sensitivity of 0.900, a specificity of 0.857, and an accuracy of 0.868 [90]. Li et al. [91] compared the diagnostic performance between the ultrasomics-based model and the CEUS Liver Imaging Reporting and Data System (LI-RADS) v2017. The ultrasomics model achieved a better sensitivity than LI-RADS (90.6% vs. 81.3%) and a better accuracy (90% vs. 83%). No differences were found on specificity and AUC. Although the results were encouraging, the ability to differentiate ICC from HCC remains low [92].

The ultrasound radiomic signature was also helpful to predict the biological characteristics of ICC. Peng et al. showed moderate efficiency in predicting the biological behaviors of 128 ICC, evaluating six pathological features. They reached the best results predicting ki67, VEGF, and CK7 (0.848, 0.864, and 0.789, respectively). Ki67 also achieved the best sensitivity, at 0.957, but a specificity of 0.500 [93].

The results obtained by the ultrasomics model are still related to clinical data and may be influenced by the operator who acquires the images [88]. Concerning differential diagnosis, the ultrasomics model can improve the diagnostic accuracy of radiologists in the characterization of liver lesions, especially in cases of underlying liver disease [94].

Although the results of the ultrasomics model compared with LI-RADS were encouraging, the difference between the two scores in the ability to differentiate ICC from HCC was not significant [92]. The data obtained on liver ultrasomics were similar to those obtained on thyroid, breast, or kidney ultrasomics [95–101].

Radiogenomics is an emerging research field that aims to correlate imaging features with the underlying genes or mutated genes [102,103]. Though most of these studies have been based on CT or MRI radiomics tools, ultrasomics has also been used especially for breast cancer, not only for the diagnosis of the lesions, but also for the prediction of the molecular subtype, with a reported accuracy of 95% [104–107].

As for the other applications of ultrasomics, for liver cancer, it is also possible to identify the limitations that currently hinder its translation into clinical practice, as there is a need for prospective multicentric studies and for automatizing the expression of results.

3.2. Computed Tomography

Mass-forming ICC usually appears at basal CT as a hypodense lesion presenting either a well-defined border or an infiltrative pattern without its own capsule (Figure 4). It is associated with heokpatic capsule retraction in about 20% of cases [108,109]. After contrast administration, the nodule shows initial peripheral rim enhancement, followed by progressive and concentric filling with contrast material as an effect of fibrosis, which is slow to enhance but retains the intravenous contrast agent [110,111].
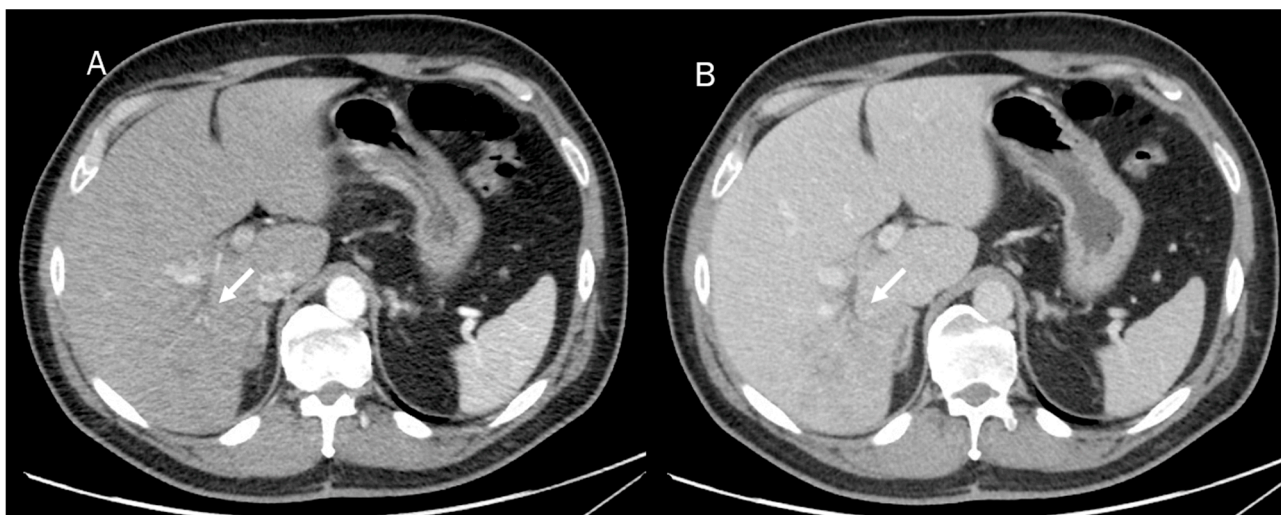
Figure 4. CT assessment of ICC (arrow) during arterial (**A**) and portal (**B**) phase of contrast study. The lesion (arrow) shows an infiltrative pattern with biliary tree dilatation.

Even though the specificity of conventional CT in characterizing lesions may appear comparable to CEUS, CT is still mandatory in pre-surgical settings to value lesion relationships with major vessels and to quantify its volume [112].

In the era of technologies innovation, dual-energy CT (DECT) based on iodine quantification can serve as a tool to improve the diagnostic accuracy of the standard CT for the differentiation of ICC and HCC [113].

Regardless of the technology used, CT evaluation of cirrhotic livers remains a challenge for radiologists due to the development of fibrous and regenerative tissue that causes the distortion of normal liver parenchyma [114,115]. This can cause a misdiagnosis of ICC, HCC, and cHCC-ICC or even hinder differentiation between malignant and benign lesions [116,117]. In the literature, these misleading patterns were reported in 5–10% of patients [118,119].

For all these reasons, several studies have proposed AI models based on CT features to correctly classify liver lesions, avoid more invasive procedures, and choose the correct timing of further radiation doses [119–121]. The majority of the enrolled studies

focused on diagnosis of ICC, cHCC-ICC, and HCC, and they did not include any rare liver disease [122–124]. Reviewing these studies, it was possible to conclude that all the radiomics tools are based on machine learning. The sample of patients included and analyzed strongly conditioned results; therefore, studies with a small sample of patients/groups needed further external validation [125–133]. However, despite the technical limitations associated with the need for a manual definition of ROIs in more than one contrast phase, radiomics models allowed promising results to be obtained. The two studies that were considered more reliable due to the larger patient sample are those of Zhou et al. [131] and Yasaka et al. [132]. Zhou et al. assessed 616 nodules, including malignant lesions (HCC, ICC, and metastasis) and benign lesions (hemangioma, focal nodular hyperplasia, and cyst) using a deep-learning approach (accuracy of 73.4%) [131]. Similar results were obtained by Yasaka et al. on 460 patients classified as having liver lesions using deep-learning (CNN) applied to CT images in the arterial and delayed phases [132]. With regard to rare hepatic lesions, an interesting study analyzed an ML approach in differential diagnosis between hepatic lymphoma (HL) and ICC [133]. The model showed a good performance and high accuracy; however; these results are less reproducible since the HL group was composed of 28 patients. Further study with external validation is expected [133].

With regard to the ICC risk assessment, recently, intrahepatic lithiasis (IHL) has been related to the development of ICC, with a conversion rate estimated between 2.4 and 13.0% [134–136]. It is very difficult for clinicians and radiologists to identify ICC hidden behind IHL because there are no specific symptoms or radiological features [137–143]. Tissue biopsy is not routinely recommended, and its negative result does not exclude the presence of malignancies [137]. Therefore, the current diagnostic accuracy of IHL-ICC is low, generally ranging from 30 to 65%. Xue et al. assessed 131 at-risk patients, showing a good performance by using a rad-score combined with a clinical-radiological model [136].

With regard to the ability of radiomics in the prediction of recurrence after treatment, several studies used preoperative or post-operative features [144–150]. Jolissant et al. predicted ICC recurrence 1 year after surgical treatment by building a model on texture features (TFs) extracted from the liver, from the tumor, and from the future liver remnant (FLR) on preoperative images [145]. Patients with early recurrence had a larger tumor size and a higher rate of lymph node metastasis (LNM) but were not more likely to have multifocal disease (21.4% vs. 17.4%, p = 0.643). The combined model with texture features and tumor size achieved the highest AUC of 0.84 (95% CI 0.73–0.95) in predicting recurrence in the validation cohort [145]. Similar results were obtained by Zhu et al. [147]. Their model was built on a logistic regression that combined preoperative and pathological features (solitary, size, differentiation, membrane invasion, portal venous phase CT value mean, equilibrium phase CT value mean, energy ap, inertia ap, percentile50th-portal phase value) and showed high diagnostic performance in terms of sensitivity (0.818) and specificity (0.909) [147].

The study by Chu et al. was the first study based on surgical technique with the aim of avoiding futile resection in high-risk-recurrence ICC. They achieved a sensitivity of 0.846 and a specificity of 0.771 in the validation cohort, comparable with previous studies. Futile resections are related to the impossibility of performing an R0 resection due to a discrepancy between preoperative evaluations and intraoperative findings. Because 16% of patients risk futile resection, the study had a clear application in clinical practice [150].

Proper patient management requires a correct disease stage assessment and a critical lymph nodes assessment to plan the correct treatment strategy and surgical approach. At present, the limit of conventional imaging for a pre-surgical-nodes-involvement evaluation is known, so great attention is being shown toward radiomics [140,151,152]. Ji et al. [140] and Zhang et al. [152] proposed a methodology to predict lymph node (LN) metastasis of ICC and to determine its prognostic value, obtaining similar results on a validation cohort [140,152].

Biological characteristics related to poor prognosis were also evaluated [153,154]. Isocitrate dehydrogenase (IDH) is frequently mutated in ICC (10–28%) and holds great

prognostic significance. Zhu et al. predicted this mutation through CT-radiomics features (a global accuracy of 0.863 and an AUC of 0.813) [155].

Although differential diagnosis with high accuracy is considered a hot topic for radiomics studies, prospective and multicentric studies are needed to validate the models. In fact, the sample of each group impacts the reliability achieved by the ML tool [125–130]. The models proposed are built on analyses with huge variability and need to be standardized. Furthermore, CT image texture analysis needs the definition of a precise ROI, excluding vessels, bile ducts, and colliquative areas or calcification; therefore, to validate the model in clinical practice, an automatization of the ROI or VOI definition is mandatory to reduce the work time [135–140].

In addition, the prediction of the lymph nodes involved can have effects in clinical practice. In fact, early recurrence and involvement of lymph nodes impact the choice of liver transplantation for unresectable ICC despite medical therapy [156–158]. Precision medicine, and consequently precision oncology, like precision surgery, should be based on these features not immediately visible to the human eye [159–162]. Therefore, there is a need for advanced technologies such as radiomics, target therapy, and minimally invasive liver surgery [163–176].

3.3. Magnetic Resonance Imaging

In the current clinical practice, MRI is performed in association with CT as standard of care to complete the study pre-treatment of cholangiocarcinoma, to evaluate the invasion of bordering structure or soft tissue, bile duct, and blood flow and the vascular morphology in the portal venous system [177–180].

In MRI imaging, ICC presents typical features as capsular retraction adjacent to the tumor. In T1-W sequences, the lesion appears with a targetoid aspect or hypointense signal. While most of the lesions also appear targetoid (Figure 5) in T2 sequences, some can show hyperintense signals. After contrast administration in the arterial phase in ICC, it is possible to identify the peripheral rim hyperenhanced. In the portal phase, the lesion slowly increases its entire enhancement (Figures 5 and 6) [181–184].
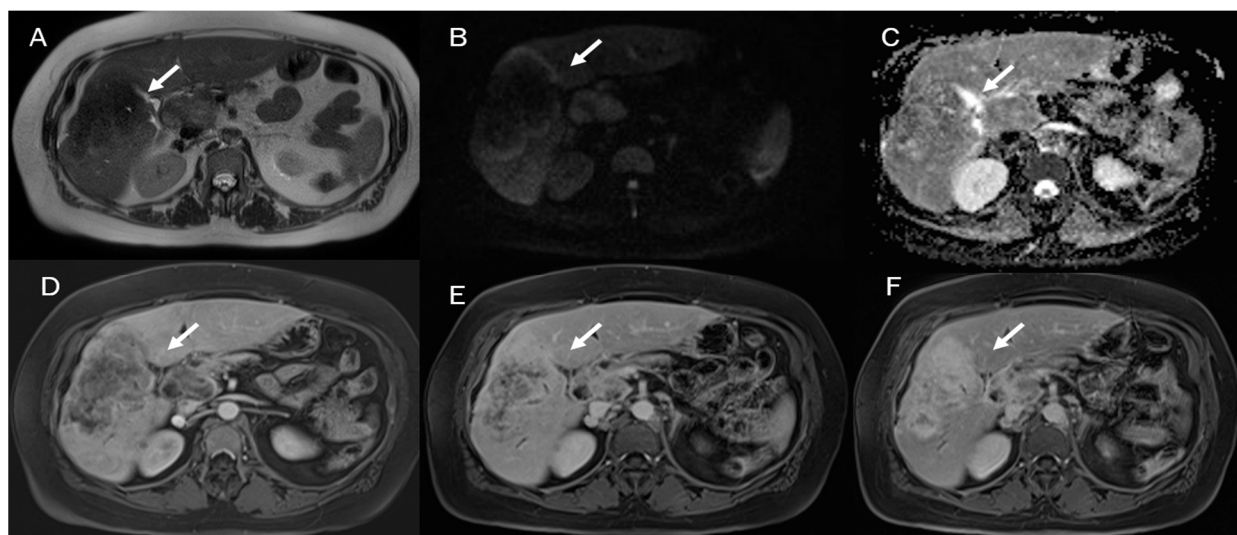
Figure 5. ICC MRI assessment. The lesion (arrow) shows hypointense signal in T2-W sequence (**A**) due to fibrotic tissue, with targetoid appearance in DWI (**B**) and ADC map (**C**) and progressive contrast enhancement during arterial (**D**), portal (**E**), and delay (**F**) phases of contrast study.
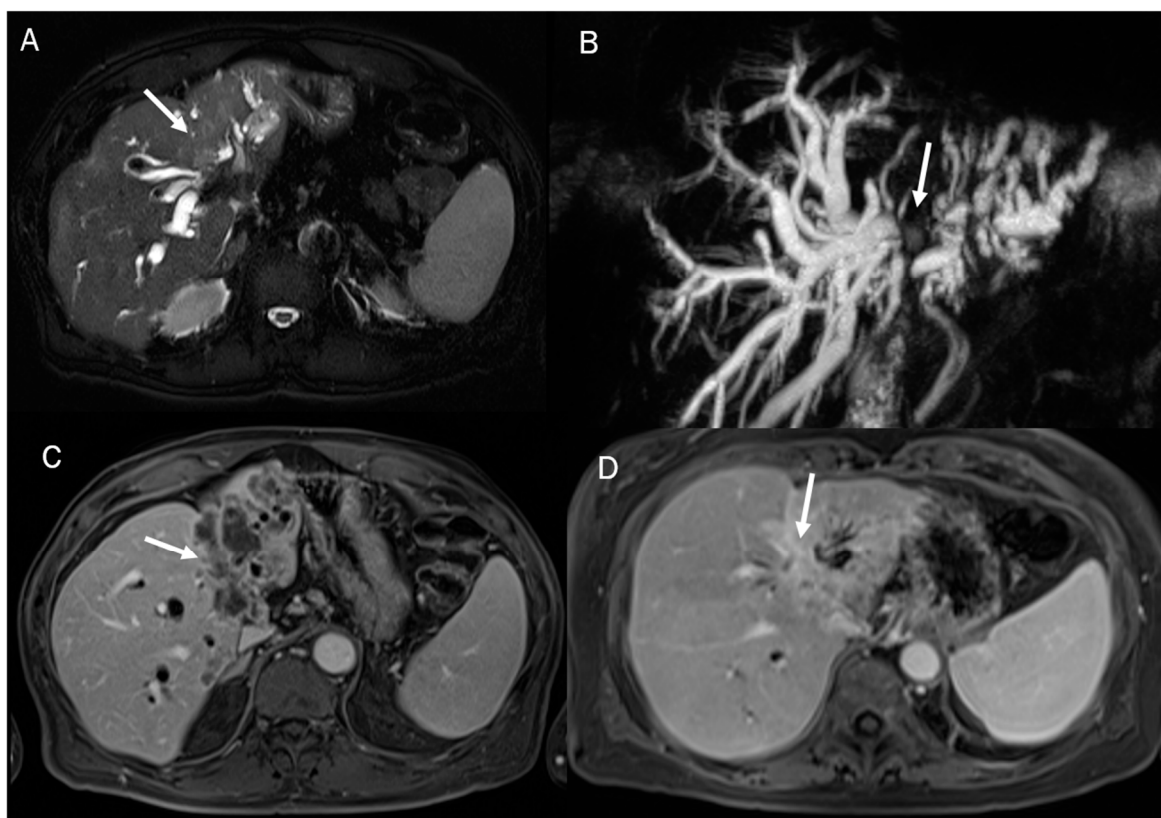
Figure 6. MRI assessment of periductal-infiltrating CCA. The lesion (arrow) shows hyperintense signal in T2-W (**A**), causing biliary tree dilatation in cholangiography sequences (**B**). During arterial phase (**C**), the lesion causes hyperenhancement of surrounding liver parenchymal, showing a progressive contrast enhancement in portal phase (**D**).

A hepatocyte-specific contrast agent, gadolinium ethoxybenzyl diethylenetriamine pentaacetic acid (Gd-EOB-DTPA), enhances the blood pool and is hepatocyte specific, since it is taken up by hepatocytes and excreted into the biliary tract (EOB phase). Approximately 50% of the administered dose of Gd-EOB-DTPA is taken up by normal hepatocytes and subsequently excreted into the biliary tract, while the remaining 50% is excreted via the kidney. Hepatocellular uptake is considered to represent passive diffusion mediated by organic anion transporter polypeptide 1 (OATP1), which is expressed on the hepatocyte membrane. Gd-EOB-DTPA-enhanced MRI may offer a breakthrough for the diagnosis of liver tumors. In the EOB phase, ICC has a hypointense signal, although considering fibrotic structure, part of the administrated dose could be detected inside the lesion. In addition, the possibility of using this type of agent to assess the ICC microenvironment could help in the treatment decision phase [6,181]. The CCA tumor microenvironment is a dynamic environment consisting of authoritative tumor stromal cells and an extracellular matrix where tumor stromal cells and cancer cells can thrive. CCA stromal cells include immune and non-immune cells, such as inflammatory cells, endothelial cells, fibroblasts, and macrophages. Likewise, the CCA tumor microenvironment contains abundant proliferative factors and can significantly impact the behavior of cancer cells. Through abominably intricate interactions with CCA cells, the CCA tumor microenvironment plays an important role in promoting tumor proliferation, accelerating neovascularization, facilitating tumor invasion, and preventing tumor cells from organismal immune reactions and apoptosis [179–181].

As for CT, the MRI-based tool achieved high accuracy in differential diagnosis among liver lesions, especially HCC and ICC. Most of the studies were conducted through machine-learning-based tools [185].

Concerning differential diagnosis, the sensitivity of gadoxetic acid-enhanced MRI should not be influenced by underlying chronic liver disease, but rather by hypervascular tumors [185]. Radiomics applied to multiphasic MRI achieved great results. A large training cohort composed of 494 lesions and a test cohort of 60 lesions achieved a sensitivity of 88% in classifying the lesions [186,187]. These results were supported by Zhou et al. (AUC of 0.80), who included ICC and cHCC-ICC [188].

In addition, in T2-W MRI images, Huang et al. proposed a methodology able to differentiate HCC from ICC in 174 patients (113 cases of HCC and 61 cases of mass-type ICCA). The AUC of the radiomics nomogram was 0.97 in the training group and 0.95 in the validation group. The results are comparable to those obtained with post contrast sequences [189].

Recent advances in machine learning brought an automatization of the model to accelerate workflow, enhance performance, and increase the accessibility of AI to clinical researchers [190]. Hu et al.'s study through auto ML achieved an accuracy similar to that of manual optimization with a sensitivity and specificity comparable to that of radiologists. However, automated ML needs to be improved on the diagnosis of LR-M of LI-RADS and needs additional features to be implemented [190,191].

The studies conducted on MRI images achieved a stronger diagnostic power than those on CT images, but prospective and multicentric studies are needed [131,132,187,188].

The theme of recurrence was also explored through MRI. The results achieved were comparable to the ones achieved by CT images analysis [192–196]. In the study by Xu et al., to predict early and late recurrence, features were extracted from the intratumoral and peritumoral area. The combined model obtained an AUC of 0.852. The early recurrence was also predicted by using post-contrast sequences, combining radiological features and immunohistochemical markers (AUC of 0.949, sensitivity of 0.875, and specificity of 0.774) [192].

With regard to nodal involvement, Xu et al. tested a model to identify lymph node metastasis in 106 patients with ICC, showing a good discrimination in separating patients with nodal metastases and without nodal involvement LNM and non-LNM (AUC: the training group: 0.842 vs. 0.788; the validation group: 0.870 vs. 0.787) [194].

With regard to prognostic assessment, several authors assessed the ability of radiomics in determining molecular characteristics, mutational status, and microvascular invasion (MVI).

Zhang et al. proposed a model to investigate the expression of PD-1/PD-L1 in ICC. The model was built on MRI images in the arterial and portal vein phases of 98 patients. The highest area under the curves of the models predicting PD-1 and PD-L1 expression was 0.897 and 0.890, respectively [197]. Zhou et al. developed a model on DCE-MRI to predict MVI in mass-forming ICC patients. Larger tumor size and higher radiomics scores were positively correlated with MVI in both the training cohort ($p < 0.001$, <0.001, respectively) and the validation cohort ($p = 0.008$, 0.001, respectively). The radiomics signature showed optimal prediction performance in validation cohorts (AUC of 0.850) [198]. Similar results were obtained by Qian et al. (AUC of 0.819 in the test cohort) for the MVI prediction model, which incorporated tumor size and intrahepatic duct dilatation [199].

Regarding MRI and radiomics, although the results are promising, several questions remain open regarding the sample under examination in terms of population homogeneity and external validations. The use of study protocols and different equipment make the results not very reproducible. In addition, some authors proposed an analysis based on DCE-MRI, where it concerns studies of CE-MRI, since they assessed specific contrast phases as arterial or portal. The optimization of the protocols could certainly lead to a greater robustness of the results.

4. Conclusions

Advances in artificial intelligence must be interpreted with caution. Virtually all studies about AI were made retrospectively, and more research is needed to make sure than the use of AI provides equivalent results in real-world prospective studies [200].

Many performing models have been developed to make differential diagnosis easier for radiologists and offer the chance to predict recurrence and genomic patterns. However, we have to underline that all the studies were retrospective, lacking further external validation in prospective and multicentric cohorts. Furthermore, the radiomics models and their expression of results should be standardized and automatized to be applicable in clinical practice.

References

1. Capuozzo, M.; Santorsola, M.; Landi, L.; Granata, V.; Perri, F.; Celotto, V.; Gualillo, O.; Nasti, G.; Ottaiano, A. Evolution of Treatment in Advanced Cholangiocarcinoma: Old and New towards Precision Oncology. *Int. J. Mol. Sci.* **2022**, *23*, 15124. [CrossRef] [PubMed]

2. Di Benedetto, F.; Magistri, P.; Guerrini, G.P.; Di Sandro, S. Robotic liver partition and portal vein embolization for staged hepatectomy for perihilar cholangiocarcinoma. *Updates Surg.* **2022**, *74*, 773–777. [CrossRef] [PubMed]

3. Saha, S.K.; Zhu, A.X.; Fuchs, C.S.; Brooks, G.A. Forty-Year Trends in Cholangiocarcinoma Incidence in the U.S.: Intrahepatic Disease on the Rise. *Oncologist* **2016**, *21*, 594–599. [CrossRef] [PubMed]

4. Granata, V.; Fusco, R.; Belli, A.; Borzillo, V.; Palumbo, P.; Bruno, F.; Grassi, R.; Ottaiano, A.; Nasti, G.; Pilone, V.; et al. Correction: Conventional, functional and radiomics assessment for intrahepatic cholangiocarcinoma. *Infect. Agent Cancer* **2022**, *17*, 22, Erratum in *Infect. Agent Cancer* **2022**, *17*, 13. [CrossRef] [PubMed]

5. Vijgen, S.; Terris, B.; Rubbia-Brandt, L. Pathology of intrahepatic cholangiocarcinoma. *Hepatobiliary Surg. Nutr.* **2017**, *6*, 22–34. [CrossRef] [PubMed]

6. Granata, V.; Grassi, R.; Fusco, R.; Setola, S.V.; Belli, A.; Ottaiano, A.; Nasti, G.; La Porta, M.; Danti, G.; Cappabianca, S.; et al. Intrahepatic cholangiocarcinoma and its differential diagnosis at MRI: How radiologist should assess MR features. *Radiol. Med.* **2021**, *126*, 1584–1600. [CrossRef]

7. Seok, J.Y.; Na, D.C.; Woo, H.G.; Roncalli, M.; Kwon, S.M.; Yoo, J.E.; Ahn, E.Y.; Kim, G.I.; Choi, J.S.; Kim, Y.B.; et al. A fibrous stromal component in hepatocellular carcinoma reveals a cholangiocarcinoma-like gene expression trait and epithelial-mesenchymal transition. *Hepatology* **2012**, *55*, 1776–1786. [CrossRef]

8. Lewis, S.; Besa, C.; Wagner, M.; Jhaveri, K.; Kihira, S.; Zhu, H.; Sadoughi, N.; Fischer, S.; Srivastava, A.; Yee, E.; et al. Prediction of the histopathologic findings of intrahepatic cholangiocarcinoma: Qualitative and quantitative assessment of diffusion-weighted imaging. *Eur. Radiol.* **2018**, *28*, 2047–2057. [CrossRef]

9. Machairas, N.; Kostakis, I.D.; Schizas, D.; Kykalos, S.; Nikiteas, N.; Sotiropoulos, G.C. Meta-analysis of laparoscopic versus open liver resection for intrahepatic cholangiocarcinoma. *Updates Surg.* **2021**, *73*, 59–68. [CrossRef]

10. Marino, R.; Ratti, F.; Catena, M.; Aldrighetti, L. Portal vein arterialization: A possibility in cholangiocarcinomas infiltrating the right hepatic artery? *Updates Surg.* **2022**, *74*, 1781–1786. [CrossRef]

11. Vicini, S.; Bortolotto, C.; Rengo, M.; Ballerini, D.; Bellini, D.; Carbone, I.; Preda, L.; Laghi, A.; Coppola, F.; Faggioni, L. A narrative review on current imaging applications of artificial intelligence and radiomics in oncology: Focus on the three most common cancers. *Radiol. Med.* **2022**, *127*, 819–836. [CrossRef] [PubMed]

12. Mazzella, A.; Bertolaccini, L.; Sedda, G.; Prisciandaro, E.; Loi, M.; Iacono, G.L.; Spaggiari, L. Pneumonectomy and broncho-pleural fistula: Predicting factors and stratification of the risk. *Updates Surg.* **2022**, *74*, 1471–1478. [CrossRef]

13. Xia, D.; Chen, G.; Wu, K.; Yu, M.; Zhang, Z.; Lu, Y.; Xu, L.; Wang, Y. Research progress and hotspot of the artificial intelligence application in the ultrasound during 2011–2021: A bibliometric analysis. *Front. Public Health* **2022**, *10*, 990708. [CrossRef] [PubMed]

14. Scapicchio, C.; Gabelloni, M.; Barucci, A.; Cioni, D.; Saba, L.; Neri, E. A deep look into radiomics. *Radiol. Med.* **2021**, *126*, 1296–1311. [CrossRef]

15. Rocca, A.; Brunese, M.C.; Santone, A.; Avella, P.; Bianco, P.; Scacchi, A.; Scaglione, M.; Bellifemine, F.; Danzi, R.; Varriano, G.; et al. Early Diagnosis of Liver Metastases from Colorectal Cancer through CT Radiomics and Formal Methods: A Pilot Study. *J. Clin. Med.* **2021**, *11*, 31. [CrossRef]

16. Brunese, L.; Mercaldo, F.; Reginelli, A.; Santone, A. Formal methods for prostate cancer Gleason score and treatment prediction using radiomic biomarkers. *Magn. Reson. Imaging* **2020**, *66*, 165–175. [CrossRef] [PubMed]

17. Brunese, L.; Brunese, M.C.; Carbone, M.; Ciccone, V.; Mercaldo, F.; Santone, A. Automatic PI-RADS assignment by means of formal methods. *Radiol. Med.* **2022**, *127*, 83–89. [CrossRef]

18. Santone, A.; Brunese, M.C.; Donnarumma, F.; Guerriero, P.; Mercaldo, F.; Reginelli, A.; Miele, V.; Giovagnoni, A.; Brunese, L. Radiomic features for prostate cancer grade detection through formal verification. *Radiol. Med.* **2021**, *126*, 688–697. [CrossRef]

19. Haghbin, H.; Aziz, M. Artificial intelligence and cholangiocarcinoma: Updates and prospects. *World J. Clin. Oncol.* **2022**, *13*, 125–134. [CrossRef]

20. Yao, F.; Bian, S.; Zhu, D.; Yuan, Y.; Pan, K.; Pan, Z.; Feng, X.; Tang, K.; Yang, Y. Machine learning-based radiomics for multiple primary prostate cancer biological characteristics prediction with ^{18}F-PSMA-1007 PET: Comparison among different volume segmentation thresholds. *Radiol. Med.* **2022**, *127*, 1170–1178. [CrossRef]

21. Cacciamani, G.E.; Sanford, D.I.; Chu, T.N.; Kaneko, M.; De Castro Abreu, A.L.; Duddalwar, V.; Gill, I.S. Is Artificial Intelligence Replacing Our Radiology Stars? Not Yet! *Eur. Urol. Open Sci.* **2022**, *48*, 14–16. [CrossRef] [PubMed]

22. Billet, N.; Grégory, J.; Ronot, M. MRI appearance of combined hepatocellular cholangiocarcinoma. *Diagn. Interv. Imaging* **2022**, *103*, 625–626. [CrossRef]

23. Capretti, G.; Bonifacio, C.; De Palma, C.; Nebbia, M.; Giannitto, C.; Cancian, P.; Laino, M.E.; Balzarini, L.; Papanikolaou, N.; Savevski, V.; et al. A machine learning risk model based on preoperative computed tomography scan to predict postoperative outcomes after pancreatoduodenectomy. *Updates Surg.* **2022**, *74*, 235–243. [CrossRef] [PubMed]

24. Cellina, M.; Pirovano, M.; Ciocca, M.; Gibelli, D.; Floridi, C.; Oliva, G. Radiomic analysis of the optic nerve at the first episode of acute optic neuritis: An indicator of optic nerve pathology and a predictor of visual recovery? *Radiol. Med.* **2021**, *126*, 698–706. [CrossRef]

25. Dong, Z.; Chen, X.; Cheng, Z.; Luo, Y.; He, M.; Chen, T.; Zhang, Z.; Qian, X.; Chen, W. Differential diagnosis of pancreatic cystic neoplasms through a radiomics-assisted system. *Front. Oncol.* **2022**, *12*, 941744. [CrossRef]

26. Marte, G.; Scuderi, V.; Rocca, A.; Surfaro, G.; Migliaccio, C.; Ceriello, A. Laparoscopic splenectomy: A single center experience. Unusual cases and expanded inclusion criteria for laparoscopic approach. *Updates Surg.* **2013**, *65*, 115–119. [CrossRef]

27. Gitto, S.; Bologna, M.; Corino, V.D.A.; Emili, I.; Albano, D.; Messina, C.; Armiraglio, E.; Parafioriti, A.; Luzzati, A.; Mainardi, L.; et al. Diffusion-weighted MRI radiomics of spine bone tumors: Feature stability and machine learning-based classification performance. *Radiol. Med.* **2022**, *127*, 518–525. [CrossRef] [PubMed]

28. Satake, H.; Ishigaki, S.; Ito, R.; Naganawa, S. Radiomics in breast MRI: Current progress toward clinical application in the era of artificial intelligence. *Radiol. Med.* **2022**, *127*, 39–56. [CrossRef]

29. Komici, K.; Bianco, A.; Perrotta, F.; Dello Iacono, A.; Bencivenga, L.; D'Agnano, V.; Rocca, A.; Bianco, A.; Rengo, G.; Guerra, G. Clinical Characteristics, Exercise Capacity and Pulmonary Function in Post-COVID-19 Competitive Athletes. *J. Clin. Med.* **2021**, *10*, 3053. [CrossRef]

30. Amato, B.; Compagna, R.; Rocca, A.; Bianco, T.; Milone, M.; Sivero, L.; Vigliotti, G.; Amato, M.; Danzi, M.; Aprea, G.; et al. Fondaparinux vs warfarin for the treatment of unsuspected pulmonary embolism in cancer patients. *Drug Des. Devel. Ther.* **2016**, *10*, 2041–2046. [CrossRef]

31. Kao, Y.S.; Lin, K.T. A meta-analysis of the diagnostic test accuracy of CT-based radiomics for the prediction of COVID-19 severity. *Radiol. Med.* **2022**, *127*, 754–762. [CrossRef] [PubMed]

32. Giuliani, A.; Avella, P.; Segreto, A.L.; Izzo, M.L.; Buondonno, A.; Coluzzi, M.; Cappuccio, M.; Brunese, M.C.; Vaschetti, R.; Scacchi, A.; et al. Postoperative Outcomes Analysis After Pancreatic Duct Occlusion: A Safe Option to Treat the Pancreatic Stump After Pancreaticoduodenectomy in Low-Volume Centers. *Front. Surg.* **2021**, *8*, 804675. [CrossRef] [PubMed]

33. Grassi, R.; Belfiore, M.P.; Montanelli, A.; Patelli, G.; Urraro, F.; Giacobbe, G.; Fusco, R.; Granata, V.; Petrillo, A.; Sacco, P.; et al. COVID-19 pneumonia: Computer-aided quantification of healthy lung parenchyma, emphysema, ground glass and consolidation on chest computed tomography (CT). *Radiol. Med.* **2021**, *126*, 553–560. [CrossRef]

34. Buondonno, A.; Avella, P.; Cappuccio, M.; Scacchi, A.; Vaschetti, R.; Di Marzo, G.; Maida, P.; Luciani, C.; Amato, B.; Brunese, M.C.; et al. A Hub and Spoke Learning Program in Bariatric Surgery in a Small Region of Italy. *Front. Surg.* **2022**, *9*, 855527. [CrossRef]

35. Brunese, L.; Mercaldo, F.; Reginelli, A.; Santone, A. Explainable Deep Learning for Pulmonary Disease and Coronavirus COVID-19 Detection from X-rays. *Comput. Methods Programs Biomed.* **2020**, *196*, 105608. [CrossRef] [PubMed]

36. Cardobi, N.; Benetti, G.; Cardano, G.; Arena, C.; Micheletto, C.; Cavedon, C.; Montemezzi, S. CT radiomic models to distinguish COVID-19 pneumonia from other interstitial pneumonias. *Radiol. Med.* **2021**, *126*, 1037–1043. [CrossRef]

37. Baeza, S.; Gil, D.; Garcia-Olivé, I.; Salcedo-Pujantell, M.; Deportós, J.; Sanchez, C.; Torres, G.; Moragas, G.; Rosell, A. A novel intelligent radiomic analysis of perfusion SPECT/CT images to optimize pulmonary embolism diagnosis in COVID-19 patients. *EJNMMI Phys.* **2022**, *9*, 84. [CrossRef]

38. Rizzetto, F.; Berta, L.; Zorzi, G.; Cincotta, A.; Travaglini, F.; Artioli, D.; Nerini Molteni, S.; Vismara, C.; Scaglione, F.; Torresin, A.; et al. Diagnostic Performance in Differentiating COVID-19 from Other Viral Pneumonias on CT Imaging: Multi-Reader Analysis Compared with an Artificial Intelligence-Based Model. *Tomography* **2022**, *8*, 2815–2827. [CrossRef]

39. Liu, J.; Wang, C.; Guo, W.; Zeng, P.; Liu, Y.; Lang, N.; Yuan, H. A preliminary study using spinal MRI-based radiomics to predict high-risk cytogenetic abnormalities in multiple myeloma. *Radiol. Med.* **2021**, *126*, 1226–1235. [CrossRef]

40. Mercaldo, F.; Brunese, M.C.; Merolla, F.; Rocca, A.; Zappia, M.; Santone, A. Prostate Gleason Score Detection by Calibrated Machine Learning Classification through Radiomic Features. *Appl. Sci.* **2022**, *12*, 11900. [CrossRef]

41. van der Lubbe, M.F.J.A.; Vaidyanathan, A.; de Wit, M.; van den Burg, E.L.; Postma, A.A.; Bruintjes, T.D.; Bilderbeek-Beckers, M.A.L.; Dammeijer, P.F.M.; Bossche, S.V.; Van Rompaey, V.; et al. A non-invasive, automated diagnosis of Menière's disease using radiomics and machine learning on conventional magnetic resonance imaging: A multicentric, case-controlled feasibility study. *Radiol. Med.* **2022**, *127*, 72–82. [CrossRef]

42. van der Lubbe, M.F.J.A.; Vaidyanathan, A.; de Wit, M.; van den Burg, E.L.; Postma, A.A.; Bruintjes, T.D.; Bilderbeek-Beckers, M.A.L.; Dammeijer, P.F.M.; Bossche, S.V.; Van Rompaey, V.; et al. Response to the letter to the editor on the article: A non-invasive, automated diagnosis of Menière's disease using radiomics and machine learning on conventional magnetic resonance imaging-a multicentric, case-controlled feasibility study. *Radiol. Med.* **2022**, *127*, 1059–1061. [CrossRef]

43. Mori, M.; Palumbo, D.; De Cobelli, F.; Fiorino, C. Does radiomics play a role in the diagnosis, staging and re-staging of gastroesophageal junction adenocarcinoma? *Updates Surg.* **2022**, *75*, 273–279. [CrossRef] [PubMed]

44. Javed, S.; Qureshi, T.A.; Gaddam, S.; Wang, L.; Azab, L.; Wachsman, A.M.; Chen, W.; Asadpour, V.; Jeon, C.Y.; Wu, B.; et al. Risk prediction of pancreatic cancer using AI analysis of pancreatic subregions in computed tomography images. *Front. Oncol.* **2022**, *12*, 1007990. [CrossRef] [PubMed]

45. Bianconi, F.; Palumbo, I.; Fravolini, M.L.; Chiari, R.; Minestrini, M.; Brunese, L.; Palumbo, B. Texture Analysis on [^{18}F]FDG PET/CT in Non-Small-Cell Lung Cancer: Correlations Between PET Features, CT Features, and Histological Types. *Mol. Imaging Biol.* **2019**, *21*, 1200–1209. [CrossRef] [PubMed]

46. Chiti, G.; Grazzini, G.; Flammia, F.; Matteuzzi, B.; Tortoli, P.; Bettarini, S.; Pasqualini, E.; Granata, V.; Busoni, S.; Messserini, L.; et al. Gastroenteropancreatic neuroendocrine neoplasms (GEP-NENs): A radiomic model to predict tumor grade. *Radiol. Med.* **2022**, *127*, 928–938. [CrossRef] [PubMed]

47. Li, S.; Zhou, B. A review of radiomics and genomics applications in cancers: The way towards precision medicine. *Radiat. Oncol.* **2022**, *17*, 217. [CrossRef]

48. Caruso, D.; Polici, M.; Rinzivillo, M.; Zerunian, M.; Nacci, I.; Marasco, M.; Magi, L.; Tarallo, M.; Gargiulo, S.; Iannicelli, E.; et al. CT-based radiomics for prediction of therapeutic response to Everolimus in metastatic neuroendocrine tumors. *Radiol. Med.* **2022**, *127*, 691–701. [CrossRef]

49. Giannini, V.; Rosati, S.; Defeudis, A.; Balestra, G.; Vassallo, L.; Cappello, G.; Mazzetti, S.; De Mattia, C.; Rizzetto, F.; Torresin, A.; et al. Radiomics predicts response of individual HER2-amplified colorectal cancer liver metastases in patients treated with HER2-targeted therapy. *Int. J. Cancer* **2020**, *147*, 3215–3223. [CrossRef]

50. Gao, W.; Wang, W.; Song, D.; Yang, C.; Zhu, K.; Zeng, M.; Rao, S.X.; Wang, M. A predictive model integrating deep and radiomics features based on gadobenate dimeglumine-enhanced MRI for postoperative early recurrence of hepatocellular carcinoma. *Radiol. Med.* **2022**, *127*, 259–271. [CrossRef]

51. Shi, Y.; Gao, F.; Qi, Y.; Lu, H.; Ai, F.; Hou, Y.; Liu, C.; Xu, Y.; Zhang, X.; Cai, X. Computed tomography-adjusted fistula risk score for predicting clinically relevant postoperative pancreatic fistula after pancreatoduodenectomy: Training and external validation of model upgrade. *EBioMedicine* **2020**, *62*, 103096. [CrossRef]

52. Han, D.; Yu, N.; Yu, Y.; He, T.; Duan, X. Performance of CT radiomics in predicting the overall survival of patients with stage III clear cell renal carcinoma after radical nephrectomy. *Radiol. Med.* **2022**, *127*, 837–847. [CrossRef]

53. Cui, Y.; Li, Z.; Xiang, M.; Han, D.; Yin, Y.; Ma, C. Machine learning models predict overall survival and progression free survival of non-surgical esophageal cancer patients with chemoradiotherapy based on CT image radiomics signatures. *Radiat. Oncol.* **2022**, *17*, 212. [CrossRef]

54. Schlanger, D.; Graur, F.; Popa, C.; Moiș, E.; Al Hajjar, N. The role of artificial intelligence in pancreatic surgery: A systematic review. *Updates Surg.* **2022**, *74*, 417–429. [CrossRef]

55. Wang, F.H.; Zheng, H.L.; Li, J.T.; Li, P.; Zheng, C.H.; Chen, Q.Y.; Huang, C.M.; Xie, J.W. Prediction of recurrence-free survival and adjuvant therapy benefit in patients with gastrointestinal stromal tumors based on radiomics features. *Radiol. Med.* **2022**, *127*, 1085–1097. [CrossRef] [PubMed]

56. Ceccarelli, G.; Costa, G.; De Rosa, M.; Codacci Pisanelli, M.; Frezza, B.; De Prizio, M.; Bravi, I.; Scacchi, A.; Gallo, G.; Amato, B.; et al. Minimally Invasive Approach to Gastric GISTs: Analysis of a Multicenter Robotic and Laparoscopic Experience with Literature Review. *Cancers* **2021**, *13*, 4351. [CrossRef]

57. Dalal, V.; Carmicheal, J.; Dhaliwal, A.; Jain, M.; Kaur, S.; Batra, S.K. Radiomics in stratification of pancreatic cystic lesions: Machine learning in action. *Cancer Lett.* **2020**, *469*, 228–237. [CrossRef]

58. Autorino, R.; Gui, B.; Panza, G.; Boldrini, L.; Cusumano, D.; Russo, L.; Nardangeli, A.; Persiani, S.; Campitelli, M.; Ferrandina, G.; et al. Radiomics-based prediction of two-year clinical outcome in locally advanced cervical cancer patients undergoing neoadjuvant chemoradiotherapy. *Radiol. Med.* **2022**, *127*, 498–506. [CrossRef] [PubMed]

59. Santambrogio, R.; Barabino, M.; D'Alessandro, V.; Iacob, G.; Opocher, E.; Gemma, M.; Zappa, M.A. Micronvasive behaviour of single small hepatocellular carcinoma: Which treatment? *Updates Surg.* **2021**, *73*, 1359–1369. [CrossRef] [PubMed]

60. Cusumano, D.; Meijer, G.; Lenkowicz, J.; Chiloiro, G.; Boldrini, L.; Masciocchi, C.; Dinapoli, N.; Gatta, R.; Casà, C.; Damiani, A.; et al. A field strength independent MR radiomics model to predict pathological complete response in locally advanced rectal cancer. *Radiol. Med.* **2021**, *126*, 421–429. [CrossRef]

61. Chen, S.; Ren, S.; Guo, K.; Daniels, M.J.; Wang, Z.; Chen, R. Preoperative differentiation of serous cystic neoplasms from mucin-producing pancreatic cystic neoplasms using a CT-based radiomics nomogram. *Abdom. Radiol.* **2021**, *46*, 2637–2646. [CrossRef] [PubMed]

62. Wong, P.K.; Chan, I.N.; Yan, H.M.; Gao, S.; Wong, C.H.; Yan, T.; Yao, L.; Hu, Y.; Wang, Z.R.; Yu, H.H. Deep learning based radiomics for gastrointestinal cancer diagnosis and treatment: A minireview. *World J. Gastroenterol.* **2022**, *28*, 6363–6379. [CrossRef]

63. Benedetti, G.; Mori, M.; Panzeri, M.M.; Barbera, M.; Palumbo, D.; Sini, C.; Muffatti, F.; Andreasi, V.; Steidler, S.; Doglioni, C.; et al. CT-derived radiomic features to discriminate histologic characteristics of pancreatic neuroendocrine tumors. *Radiol. Med.* **2021**, *126*, 745–760. [CrossRef] [PubMed]

64. Huang, Z.; Shu, Z.; Zhu, R.H.; Xin, J.Y.; Wu, L.L.; Wang, H.Z.; Chen, J.; Zhang, Z.W.; Luo, H.C.; Li, K.Y. Deep learning-based radiomics based on contrast-enhanced ultrasound predicts early recurrence and survival outcome in hepatocellular carcinoma. *World J. Gastrointest. Oncol.* **2022**, *14*, 2380–2392. [CrossRef] [PubMed]

65. Gregucci, F.; Fiorentino, A.; Mazzola, R.; Ricchetti, F.; Bonaparte, I.; Surgo, A.; Figlia, V.; Carbonara, R.; Caliandro, M.; Ciliberti, M.P.; et al. Radiomic analysis to predict local response in locally advanced pancreatic cancer treated with stereotactic body radiation therapy. *Radiol. Med.* **2022**, *127*, 100–107. [CrossRef]

66. Sim, K.C.; Kim, M.J.; Cho, Y.; Kim, H.J.; Park, B.J.; Sung, D.J.; Han, N.Y.; Han, Y.E.; Kim, T.H.; Lee, Y.J. Radiomics Analysis of Magnetic Resonance Proton Density Fat Fraction for the Diagnosis of Hepatic Steatosis in Patients with Suspected Non-Alcoholic Fatty Liver Disease. *J. Korean Med. Sci.* **2022**, *37*, e339. [CrossRef]

67. Kotowski, K.; Kucharski, D.; Machura, B.; Adamski, S.; Gutierrez Becker, B.; Krason, A.; Zarudzki, L.; Tessier, J.; Nalepa, J. Detecting liver cirrhosis in computed tomography scans using clinically-inspired and radiomic features. *Comput. Biol. Med.* **2022**, *152*, 106378. [CrossRef]

68. Li, B.; Tai, D.I.; Yan, K.; Chen, Y.C.; Chen, C.J.; Huang, S.F.; Hsu, T.H.; Yu, W.T.; Xiao, J.; Le, L.; et al. Accurate and generalizable quantitative scoring of liver steatosis from ultrasound images via scalable deep learning. *World J. Gastroenterol.* **2022**, *28*, 2494–2508. [CrossRef]

69. Romeo, V.; Verde, F.; Sarno, L.; Migliorini, S.; Petretta, M.; Mainenti, P.P.; D'Armiento, M.; Guida, M.; Brunetti, A.; Maurea, S. Prediction of placenta accreta spectrum in patients with placenta previa using clinical risk factors, ultrasound and magnetic resonance imaging findings. *Radiol. Med.* **2021**, *126*, 1216–1225. [CrossRef]

70. Jeon, S.K.; Lee, J.M.; Joo, I.; Yoon, J.H. Assessment of the inter-platform reproducibility of ultrasound attenuation examination in nonalcoholic fatty liver disease. *Ultrasonography* **2022**, *41*, 355–364. [CrossRef]

71. Mao, Y.; Mu, J.; Zhao, J.; Yang, F.; Zhao, L. The comparative study of color doppler flow imaging, superb microvascular imaging, contrast-enhanced ultrasound micro flow imaging in blood flow analysis of solid renal mass. *Cancer Imaging* **2022**, *22*, 21. [CrossRef]

72. Ceccarelli, G.; Andolfi, E.; Fontani, A.; Calise, F.; Rocca, A.; Giuliani, A. Robot-assisted liver surgery in a general surgery unit with a "Referral Centre Hub&Spoke Learning Program". Early outcomes after our first 70 consecutive patients. *Minerva Chir.* **2018**, *73*, 460–468. [CrossRef]

73. Di Serafino, M.; Vallone, G. The role of point of care ultrasound in radiology department: Update and prospective. A statement of Italian college ultrasound. *Radiol. Med.* **2021**, *126*, 636–641. [CrossRef]

74. Aprea, G.; Rocca, A.; Salzano, A.; Sivero, L.; Scarpaleggia, M.; Ocelli, P.; Amato, M.; Bianco, T.; Serra, R.; Amato, B. Laparoscopic single site (LESS) and classic video-laparoscopic cholecystectomy in the elderly: A single centre experience. *Int. J. Surg.* **2016**, *33* (Suppl. 1), S1–S3. [CrossRef] [PubMed]

75. Barton, A. Considering the uncompliant patient: A four-step approach. *Br. J. Nurs.* **2017**, *26*, S12. [CrossRef]

76. Rocca, A.; Brunese, M.C.; Cappuccio, M.; Scacchi, A.; Martucci, G.; Buondonno, A.; Perrotta, F.M.; Quarto, G.; Avella, P.; Amato, B. Impact of Physical Activity on Disability Risk in Elderly Patients Hospitalized for Mild Acute Diverticulitis and Diverticular Bleeding Undergone Conservative Management. *Medicina* **2021**, *57*, 360. [CrossRef]

77. Ruan, S.M.; Huang, H.; Cheng, M.Q.; Lin, M.X.; Hu, H.T.; Huang, Y.; Li, M.D.; Lu, M.D.; Wang, W. Shear-wave elastography combined with contrast-enhanced ultrasound algorithm for noninvasive characterization of focal liver lesions. *Radiol. Med.* **2022**. [CrossRef] [PubMed]

78. Zhou, Y.; Yin, S.; Zhao, L.; Zhang, X.; Li, M.; Ding, J.; Yan, K.; Jing, X. CEUS and CT/MRI LI-RADS in Association with Serum Biomarkers for Differentiation of Combined Hepatocellular-Cholangiocarcinoma From Hepatocellular Carcinoma. *Front. Oncol.* **2022**, *12*, 897090. [CrossRef] [PubMed]

79. Hu, H.T.; Wang, W.; Chen, L.D.; Ruan, S.M.; Chen, S.L.; Li, X.; Lu, M.D.; Xie, X.Y.; Kuang, M. Artificial intelligence assists identifying malignant versus benign liver lesions using contrast-enhanced ultrasound. *J. Gastroenterol. Hepatol.* **2021**, *36*, 2875–2883. [CrossRef]

80. Nakanuma, Y.; Sripa, B.; Vatanasapt, V.; Leong, A.S.Y.; Ponchon, T.; Ishak, K.G. Intrahepatic cholangiocarcinoma. In *World Health Organization Classification of Tumours Pathology and Genetics of Tumours of the Digestive System*; WHO: Geneva, Switzerland, 2000; pp. 173–180.

81. Takakura, K.; Kajihara, M.; Iwasaki, T.; Ide, D.; Miyazaki, T.; Arai, Y.; Saruta, M.; Arihiro, S.; Matsuoka, M.; Koido, S.; et al. Unusual images of mass-forming intrahepatic cholangiocarcinoma. *Case Rep. Gastroenterol.* **2013**, *7*, 414–419. [CrossRef] [PubMed]

82. Vidili, G.; Arru, M.; Solinas, G.; Calvisi, D.F.; Meloni, P.; Sauchella, A.; Turilli, D.; Fabio, C.; Cossu, A.; Madeddu, G.; et al. Contrast-enhanced ultrasound Liver Imaging Reporting and Data System: Lights and shadows in hepatocellular carcinoma and cholangiocellular carcinoma diagnosis. *World J. Gastroenterol.* **2022**, *28*, 3488–3502. [CrossRef]

83. Zeng, D.; Xu, M.; Liang, J.Y.; Cheng, M.Q.; Huang, H.; Pan, J.M.; Huang, Y.; Tong, W.J.; Xie, X.Y.; Lu, M.D.; et al. Using new criteria to improve the differentiation between HCC and non-HCC malignancies: Clinical practice and discussion in CEUS LI-RADS 2017. *Radiol. Med.* **2022**, *127*, 1–10. [CrossRef]

84. Karmazanovsky, G.; Gruzdev, I.; Tikhonova, V.; Kondratyev, E.; Revishvili, A. Computed tomography-based radiomics approach in pancreatic tumors characterization. *Radiol. Med.* **2021**, *126*, 1388–1395. [CrossRef]

85. European Association for the Study of the Liver. EASL clinical practice guidelines: Management of hepatocellular carcinoma. *J. Hepatol.* **2018**, *69*, 182–236. [CrossRef] [PubMed]

86. Argalia, G.; Ventura, C.; Tosi, N.; Campioni, D.; Tagliati, C.; Tufillaro, M.; Cucco, M.; Svegliati Baroni, G.; Giovagnoni, A. Comparison of point shear wave elastography and transient elastography in the evaluation of patients with NAFLD. *Radiol. Med.* **2022**, *127*, 571–576. [CrossRef] [PubMed]

87. Chen, Y.; Zhu, Y.; Chen, K.; Wang, H.; Zhang, W.; Bao, J.; Wang, W. Differentiation between hepatocellular carcinoma and intrahepatic cholangiocarcinoma using contrast-enhanced ultrasound: A systematic review and meta-analysis. *Clin. Hemorheol. Microcirc.* **2021**, *79*, 293–309. [CrossRef]

88. Gurgitano, M.; Angileri, S.A.; Rodà, G.M.; Liguori, A.; Pandolfi, M.; Ierardi, A.M.; Wood, B.J.; Carrafiello, G. Interventional Radiology ex-machina: Impact of Artificial Intelligence on practice. *Radiol. Med.* **2021**, *126*, 998–1006. [CrossRef] [PubMed]

89. Peng, Y.; Lin, P.; Wu, L.; Wan, D.; Zhao, Y.; Liang, L.; Ma, X.; Qin, H.; Liu, Y.; Li, X.; et al. Ultrasound-Based Radiomics Analysis for Preoperatively Predicting Different Histopathological Subtypes of Primary Liver Cancer. *Front. Oncol.* **2020**, *10*, 1646. [CrossRef] [PubMed]

90. Ren, S.; Li, Q.; Liu, S.; Qi, Q.; Duan, S.; Mao, B.; Li, X.; Wu, Y.; Zhang, L. Clinical Value of Machine Learning-Based Ultrasomics in Preoperative Differentiation Between Hepatocellular Carcinoma and Intrahepatic Cholangiocarcinoma: A Multicenter Study. *Front. Oncol.* **2021**, *11*, 749137. [CrossRef]

91. Li, C.Q.; Zheng, X.; Guo, H.L.; Cheng, M.Q.; Huang, Y.; Xie, X.Y.; Lu, M.D.; Kuang, M.; Wang, W.; Chen, L.D. Differentiation between combined hepatocellular carcinoma and hepatocellular carcinoma: Comparison of diagnostic performance between ultrasomics-based model and CEUS LI-RADS v2017. *BMC Med. Imaging* **2022**, *22*, 36, Erratum in *BMC Med. Imaging.* **2022**, *22*, 57. [CrossRef]

92. Barabino, M.; Gurgitano, M.; Fochesato, C.; Angileri, S.A.; Franceschelli, G.; Santambrogio, R.; Mariani, N.M.; Opocher, E.; Carrafiello, G. LI-RADS to categorize liver nodules in patients at risk of HCC: Tool or a gadget in daily practice? *Radiol. Med.* **2021**, *126*, 5–13. [CrossRef]

93. Peng, Y.T.; Zhou, C.Y.; Lin, P.; Wen, D.Y.; Wang, X.D.; Zhong, X.Z.; Pan, D.H.; Que, Q.; Li, X.; Chen, L.; et al. Preoperative Ultrasound Radiomics Signatures for Noninvasive Evaluation of Biological Characteristics of Intrahepatic Cholangiocarcinoma. *Acad. Radiol.* **2020**, *27*, 785–797. [CrossRef]

94. Argalia, G.; Tarantino, G.; Ventura, C.; Campioni, D.; Tagliati, C.; Guardati, P.; Kostandini, A.; Marzioni, M.; Giuseppetti, G.M.; Giovagnoni, A. Shear wave elastography and transient elastography in HCV patients after direct-acting antivirals. *Radiol. Med.* **2021**, *126*, 894–899. [CrossRef] [PubMed]

95. Wen, Q.; Wang, Z.; Traverso, A.; Liu, Y.; Xu, R.; Feng, Y.; Qian, L. A radiomics nomogram for the ultrasound-based evaluation of central cervical lymph node metastasis in papillary thyroid carcinoma. *Front. Endocrinol.* **2022**, *13*, 1064434. [CrossRef]

96. Yang, R.; Wu, J.; Sun, L.; Lai, S.; Xu, Y.; Liu, X.; Ma, Y.; Zhen, X. Radiomics of small renal masses on multiphasic CT: Accuracy of machine learning-based classification models for the differentiation of renal cell carcinoma and angiomyolipoma without visible fat. *Eur Radiol.* **2020**, *30*, 1254–1263. [CrossRef]

97. Celletti, I.; Fresilli, D.; De Vito, C.; Bononi, M.; Cardaccio, S.; Cozzolino, A.; Durante, C.; Grani, G.; Grimaldi, G.; Isidori, A.M.; et al. TIRADS, SRE and SWE in INDETERMINATE thyroid nodule characterization: Which has better diagnostic performance? *Radiol. Med.* **2021**, *126*, 1189–1200. [CrossRef] [PubMed]

98. Lu, W.; Zhang, D.; Zhang, Y.; Qian, X.; Qian, C.; Wei, Y.; Xia, Z.; Ding, W.; Ni, X. Ultrasound Radiomics Nomogram to Diagnose Sub-Centimeter Thyroid Nodules Based on ACR TI-RADS. *Cancers* **2022**, *14*, 4826. [CrossRef] [PubMed]

99. Soyer Güldoğan, E.; Ergun, O.; Taşkın Türkmenoğlu, T.; Yılmaz, K.B.; Akdağ, T.; Özbal Güneş, S.; Durmaz, H.A.; Hekimoğlu, B. The impact of TI-RADS in detecting thyroid malignancies: A prospective study. *Radiol. Med.* **2021**, *126*, 1335–1344. [CrossRef]

100. Qin, H.; Que, Q.; Lin, P.; Li, X.; Wang, X.R.; He, Y.; Chen, J.Q.; Yang, H. Magnetic resonance imaging (MRI) radiomics of papillary thyroid cancer (PTC): A comparison of predictive performance of multiple classifiers modeling to identify cervical lymph node metastases before surgery. *Radiol. Med.* **2021**, *126*, 1312–1327. [CrossRef]

101. Zhang, L.; Sun, K.; Shi, L.; Qiu, J.; Wang, X.; Wang, S. Ultrasound Image-Based Deep Features and Radiomics for the Discrimination of Small Fat-Poor Angiomyolipoma and Small Renal Cell Carcinoma. *Ultrasound Med. Biol.* **2023**, *49*, 560–568. [CrossRef]

102. Cui, H.; Zhang, D.; Peng, F.; Kong, H.; Guo, Q.; Wu, T.; Wen, X.; Zhang, L.; Tian, J. Identifying ultrasound features of positive expression of Ki67 and P53 in breast cancer using radiomics. *Asia Pac. J. Clin. Oncol.* **2021**, *17*, e176–e184. [CrossRef] [PubMed]

103. Wang, Y.G.; Xu, F.J.; Agyekum, E.A.; Xiang, H.; Wang, Y.D.; Zhang, J.; Sun, H.; Zhang, G.L.; Bo, X.S.; Lv, W.Z.; et al. Radiomic Model for Determining the Value of Elasticity and Grayscale Ultrasound Diagnoses for Predicting BRAF^{V600E} Mutations in Papillary Thyroid Carcinoma. *Front. Endocrinol.* **2022**, *13*, 872153. [CrossRef] [PubMed]

104. Xu, M.L.; Zeng, S.E.; Li, F.; Cui, X.W.; Liu, G.F. Preoperative prediction of lymphovascular invasion in patients with T1 breast invasive ductal carcinoma based on radiomics nomogram using grayscale ultrasound. *Front. Oncol.* **2022**, *12*, 1071677. [CrossRef] [PubMed]

105. Guo, Y.; Wu, J.; Wang, Y.; Jin, Y. Development and Validation of an Ultrasound-Based Radiomics Nomogram for Identifying HER2 Status in Patients with Breast Carcinoma. *Diagnostics* **2022**, *12*, 3130. [CrossRef]

106. Jiang, M.; Zhang, D.; Tang, S.C.; Luo, X.M.; Chuan, Z.R.; Lv, W.Z.; Jiang, F.; Ni, X.J.; Cui, X.W.; Dietrich, C.F. Deep learning with convolutional neural network in the assessment of breast cancer molecular subtypes based on US images: A multicenter retrospective study. *Eur. Radiol.* **2021**, *31*, 3673–3682. [CrossRef]

107. Gu, J.; Jiang, T. Ultrasound radiomics in personalized breast management: Current status and future prospects. *Front. Oncol.* **2022**, *12*, 963612. [CrossRef]

108. Rimola, J.; Forner, A.; Reig, M.; Vilana, R.; de Lope, C.R.; Ayuso, C.; Bruix, J. Cholangiocarcinoma in cirrhosis: Absence of contrast washout in delayed phases by magnetic resonance imaging avoids misdiagnosis of hepatocel- lular carcinoma. *Hepatology* **2009**, *50*, 791–798. [CrossRef]

109. Chen, Y.; Pan, Y.; Shen, K.R.; Zhu, X.L.; Lu, C.Y.; Li, Q.H.; Han, S.G.; Fu, Y.B.; Xu, X.F.; Yu, R.S. Contrast-enhanced multiple-phase imaging features of intrahepatic mass-forming cholangiocarcinoma and hepatocellular carcinoma with cirrhosis: A comparative study. *Oncol. Lett.* **2017**, *14*, 4213–4219. [CrossRef]

110. Weber, S.M.; Ribero, D.; O'Reilly, E.M.; Kokudo, N.; Miyazaki, M.; Pawlik, T.M. Intrahepatic cholangiocarcinoma: Expert consensus statement. *HPB* **2015**, *17*, 669–680. [CrossRef]

111. Fábrega-Foster, K.; Ghasabeh, M.A.; Pawlik, T.M.; Kamel, I.R. Multimodality imaging of intrahepatic cholangiocarcinoma. *Hepatobiliary Surg. Nutr.* **2017**, *6*, 67–78. [CrossRef]

112. Marrero, J.A.; Kulik, L.M.; Sirlin, C.B.; Zhu, A.X.; Finn, R.S.; Abecassis, M.M.; Roberts, L.R.; Heimbach, J.K. Diagnosis, staging, and management of hepatocellular carcinoma: 2018 practice guid- ance by the American association for the study of liver diseases. *Hepatology* **2018**, *68*, 723–750. [CrossRef] [PubMed]

113. Cicero, G.; Mazziotti, S.; Silipigni, S.; Blandino, A.; Cantisani, V.; Pergolizzi, S.; D'Angelo, T.; Stagno, A.; Maimone, S.; Squadrito, G.; et al. Dual-energy CT quantification of fractional extracellular space in cirrhotic patients: Comparison between early and delayed equilibrium phases and correlation with oesophageal varices. *Radiol. Med.* **2021**, *126*, 761–767. [CrossRef] [PubMed]

114. Scialpi, M.; Palumbo, B.; Pierotti, L.; Gravante, S.; Piunno, A.; Rebonato, A.; D'Andrea, A.; Reginelli, A.; Piscioli, I.; Brunese, L.; et al. Detection and characterization of focal liver lesions by split-bolus multidetector-row CT: Diagnostic accuracy and radiation dose in oncologic patients. *Anticancer Res.* **2014**, *34*, 4335–4344. [PubMed]

115. Mahmoudi, S.; Bernatz, S.; Althoff, F.C.; Koch, V.; Grünewald, L.D.; Scholtz, J.E.; Walter, D.; Zeuzem, S.; Wild, P.J.; Vogl, T.J.; et al. Dual-energy CT based material decomposition to differentiate intrahepatic cholangiocarcinoma from hepatocellular carcinoma. *Eur. J. Radiol.* **2022**, *156*, 110556. [CrossRef]

116. Renzulli, M.; Brandi, N.; Argalia, G.; Brocchi, S.; Farolfi, A.; Fanti, S.; Golfieri, R. Morphological, dynamic and functional characteristics of liver pseudolesions and benign lesions. *Radiol. Med.* **2022**, *127*, 129–144. [CrossRef]

117. Yoon, J.; Park, S.H.; Ahn, S.J.; Shim, Y.S. Atypical Manifestation of Primary Hepatocellular Carcinoma and Hepatic Malignancy Mimicking Lesions. *J. Korean Soc. Radiol.* **2022**, *83*, 808–829. [CrossRef]

118. Nakamura, Y.; Higaki, T.; Honda, Y.; Tatsugami, F.; Tani, C.; Fukumoto, W.; Narita, K.; Kondo, S.; Akagi, M.; Awai, K. Advanced CT techniques for assessing hepatocellular carcinoma. *Radiol. Med.* **2021**, *126*, 925–935. [CrossRef]

119. Viganò, L.; Lleo, A.; Muglia, R.; Gennaro, N.; Samà, L.; Colapietro, F.; Roncalli, M.; Aghemo, A.; Chiti, A.; Di Tommaso, L.; et al. Intrahepatic cholangiocellular carcinoma with radiological enhancement patterns mimicking hepatocellular carcinoma. *Updates Surg.* **2020**, *72*, 413–421. [CrossRef]

120. Fusco, R.; Setola, S.V.; Raiano, N.; Granata, V.; Cerciello, V.; Pecori, B.; Petrillo, A. Analysis of a monocentric computed tomography dosimetric database using a radiation dose index monitoring software: Dose levels and alerts before and after the implementation of the adaptive statistical iterative reconstruction on CT images. *Radiol. Med.* **2022**, *127*, 733–742. [CrossRef] [PubMed]

121. Scialpi, M.; Moschini, T.O.; De Filippis, G. PET/contrast-enhanced CT in oncology: "to do, or not to do, that is the question". *Radiol. Med.* **2022**, *127*, 925–927. [CrossRef]

122. Rocca, A.; Calise, F.; Marino, G.; Montagnani, S.; Cinelli, M.; Amato, B.; Guerra, G. Primary giant hepatic neuroendocrine carcinoma: A case report. *Int. J. Surg.* **2014**, *12* (Suppl. 1), S218–S221. [CrossRef] [PubMed]

123. Hu, J.; Wang, Y.; Deng, L.; Yu, H.; Chen, K.; Bao, W.; Chen, K.; Chen, G. Development and validation of a nomogram for predicting the cancer-specific survival of fibrolamellar hepatocellular carcinoma patients. *Updates Surg.* **2022**, *74*, 1589–1599. [CrossRef] [PubMed]

124. Danti, G.; Flammia, F.; Matteuzzi, B.; Cozzi, D.; Berti, V.; Grazzini, G.; Pradella, S.; Recchia, L.; Brunese, L.; Miele, V. Gastrointestinal neuroendocrine neoplasms (GI-NENs): Hot topics in morphological, functional, and prognostic imaging. *Radiol. Med.* **2021**, *126*, 1497–1507. [CrossRef] [PubMed]

125. Nakai, H.; Fujimoto, K.; Yamashita, R.; Sato, T.; Someya, Y.; Taura, K.; Isoda, H.; Nakamoto, Y. Convolutional neural network for classifying primary liver cancer based on triple-phase CT and tumor marker information: A pilot study. *Jpn. J. Radiol.* **2021**, *39*, 690–702. [CrossRef] [PubMed]

126. Zhang, J.; Huang, Z.; Cao, L.; Zhang, Z.; Wei, Y.; Zhang, X.; Song, B. Differentiation combined hepatocellular and cholangiocarcinoma from intrahepatic cholangiocarcinoma based on radiomics machine learning. *Ann. Transl. Med.* **2020**, *8*, 119. [CrossRef]

127. Liu, X.; Khalvati, F.; Namdar, K.; Fischer, S.; Lewis, S.; Taouli, B.; Haider, M.A.; Jhaveri, K.S. Can machine learning radiomics provide pre-operative differentiation of combined hepatocellular cholangiocarcinoma from hepatocellular carcinoma and cholangiocarcinoma to inform optimal treatment planning? *Eur. Radiol.* **2021**, *31*, 244–255. [CrossRef]

128. Wan, Y.; Yang, P.; Xu, L.; Yang, J.; Luo, C.; Wang, J.; Chen, F.; Wu, Y.; Lu, Y.; Ruan, D.; et al. Radiomics analysis combining unsupervised learning and handcrafted features: A multiple-disease study. *Med. Phys.* **2021**, *48*, 7003–7015. [CrossRef]

129. Xu, X.; Mao, Y.; Tang, Y.; Liu, Y.; Xue, C.; Yue, Q.; Liu, Q.; Wang, J.; Yin, Y. Classification of Hepatocellular Carcinoma and Intrahepatic Cholangiocarcinoma Based on Radiomic Analysis. *Comput. Math. Methods Med.* **2022**, *2022*, 5334095. [CrossRef]

130. Matake, K.; Yoshimitsu, K.; Kumazawa, S.; Higashida, Y.; Irie, H.; Asayama, Y.; Nakayama, T.; Kakihara, D.; Katsuragawa, S.; Doi, K.; et al. Usefulness of artificial neural network for differential diagnosis of hepatic masses on CT images. *Acad. Radiol.* **2006**, *13*, 951–962. [CrossRef]

131. Zhou, J.; Wang, W.; Lei, B.; Ge, W.; Huang, Y.; Zhang, L.; Yan, Y.; Zhou, D.; Ding, Y.; Wu, J.; et al. Automatic Detection and Classification of Focal Liver Lesions Based on Deep Convolutional Neural Networks: A Preliminary Study. *Front. Oncol.* **2021**, *10*, 581210. [CrossRef]

132. Yasaka, K.; Akai, H.; Abe, O.; Kiryu, S. Deep Learning with Convolutional Neural Network for Differentiation of Liver Masses at Dynamic Contrast-enhanced CT: A Preliminary Study. *Radiology* **2018**, *286*, 887–896. [CrossRef]

133. Xu, H.; Zou, X.; Zhao, Y.; Zhang, T.; Tang, Y.; Zheng, A.; Zhou, X.; Ma, X. Differentiation of Intrahepatic Cholangiocarcinoma and Hepatic Lymphoma Based on Radiomics and Machine Learning in Contrast-Enhanced Computer Tomography. *Technol. Cancer Res. Treat.* **2021**, *20*, 15330338211039125. [CrossRef] [PubMed]

134. Lorio, E.; Patel, P.; Rosenkranz, L.; Patel, S.; Sayana, H. Management of Hepatolithiasis: Review of the Literature. *Curr. Gastroenterol. Rep.* **2020**, *22*, 30. [CrossRef] [PubMed]

135. Shen, X.; Zhao, H.; Jin, X.; Chen, J.; Yu, Z.; Ramen, K.; Zheng, X.; Wu, X.; Shan, Y.; Bai, J.; et al. Development and validation of a machine learning-based nomogram for prediction of intrahepatic cholangiocarcinoma in patients with intrahepatic lithiasis. *Hepatobiliary Surg. Nutr.* **2021**, *10*, 749–765. [CrossRef]

136. Xue, B.; Wu, S.; Zheng, M.; Jiang, H.; Chen, J.; Jiang, Z.; Tian, T.; Tu, Y.; Zhao, H.; Shen, X.; et al. Development and Validation of a Radiomic-Based Model for Prediction of Intrahepatic Cholangiocarcinoma in Patients With Intrahepatic Lithiasis Complicated by Imagologically Diagnosed Mass. *Front. Oncol.* **2021**, *10*, 598253. [CrossRef]

137. Lu, Q.; Yang, J.; Wang, P.; Liu, J.; Fan, Y.; Fang, C. Digital Surgical Diagnosis and Management of Hepatolithiasis. In *Biliary Tract Surgery*; Fang, C., Lau, W.Y., Eds.; Springer: Singapore, 2021. [CrossRef]

138. Mansour, J.C.; Aloia, T.A.; Crane, C.H.; Heimbach, J.K.; Nagino, M.; Vauthey, J.N. Hilar cholangiocarcinoma: Expert consensus statement. *HPB* **2015**, *17*, 691–699. [CrossRef]

139. Suzuki, Y.; Mori, T.; Momose, H.; Matsuki, R.; Kogure, M.; Abe, N.; Isayama, H.; Tazuma, S.; Tanaka, A.; Takikawa, H.; et al. Predictive factors for subsequent intrahepatic cholangiocarcinoma associated with hepatolithiasis: Japanese National Cohort Study for 18 years. *J. Gastroenterol.* **2022**, *57*, 387–395. [CrossRef] [PubMed]

140. Ji, G.W.; Zhu, F.P.; Zhang, Y.D.; Liu, X.S.; Wu, F.Y.; Wang, K.; Xia, Y.X.; Zhang, Y.D.; Jiang, W.J.; Li, X.C.; et al. A radiomics approach to predict lymph node metastasis and clinical outcome of intrahepatic cholangiocarcinoma. *Eur Radiol.* **2019**, *29*, 3725–3735. [CrossRef]

141. Xue, B.; Wu, S.; Zhang, M.; Hong, J.; Liu, B.; Xu, N.; Zeng, Q.; Tang, K.; Zheng, X. A radiomic-based model of different contrast-enhanced CT phase for differentiate intrahepatic cholangiocarcinoma from inflammatory mass with hepatolithiasis. *Abdom. Radiol.* **2021**, *46*, 3835–3844. [CrossRef]

142. Uenishi, T.; Hamba, H.; Takemura, S.; Oba, K.; Ogawa, M.; Yamamoto, T.; Tanaka, S.; Kubo, S. Outcomes of hepatic resection for hepatolithiasis. *Am. J. Surg.* **2009**, *198*, 199–202. [CrossRef]

143. Su, C.H.; Shyr, Y.M.; Lui, W.Y.; P'Eng, F.K. Hepatolithiasis associated with cholangiocarcinoma. *Br. J. Surg.* **1997**, *84*, 969–973. [CrossRef] [PubMed]

144. Bozkurt, M.; Eldem, G.; Bozbulut, U.B.; Bozkurt, M.F.; Kılıçkap, S.; Peynircioğlu, B.; Çil, B.; Lay Ergün, E.; Volkan-Salanci, B. Factors affecting the response to Y-90 microsphere therapy in the cholangiocarcinoma patients. *Radiol. Med.* **2021**, *126*, 323–333. [CrossRef] [PubMed]

145. Jolissaint, J.S.; Wang, T.; Soares, K.C.; Chou, J.F.; Gönen, M.; Pak, L.M.; Boerner, T.; Do, R.K.G.; Balachandran, V.P.; D'Angelica, M.I.; et al. Machine learning radiomics can predict early liver recurrence after resection of intrahepatic cholangiocarcinoma. *HPB* **2022**, *24*, 1341–1350. [CrossRef] [PubMed]

146. De Robertis, R.; Geraci, L.; Tomaiuolo, L.; Bortoli, L.; Beleù, A.; Malleo, G.; D'Onofrio, M. Liver metastases in pancreatic ductal adenocarcinoma: A predictive model based on CT texture analysis. *Radiol. Med.* **2022**, *127*, 1079–1084. [CrossRef]

147. Zhu, Y.; Mao, Y.; Chen, J.; Qiu, Y.; Guan, Y.; Wang, Z.; He, J. Radiomics-based model for predicting early recurrence of intrahepatic mass-forming cholangiocarcinoma after curative tumor resection. *Sci. Rep.* **2021**, *11*, 18347. [CrossRef]

148. Wakiya, T.; Ishido, K.; Kimura, N.; Nagase, H.; Kanda, T.; Ichiyama, S.; Soma, K.; Matsuzaka, M.; Sasaki, Y.; Kubota, S.; et al. CT-based deep learning enables early postoperative recurrence prediction for intrahepatic cholangiocarcinoma. *Sci. Rep.* **2022**, *12*, 8428. [CrossRef]

149. Hao, X.; Liu, B.; Hu, X.; Wei, J.; Han, Y.; Liu, X.; Chen, Z.; Li, J.; Bai, J.; Chen, Y.; et al. A Radiomics-based Approach for Predicting Early Recurrence in Intrahepatic Cholangiocarcinoma after Surgical Resection: A Multicenter Study. *Annu. Int. Conf. IEEE Eng. Med. Biol. Soc.* **2021**, *2021*, 3659–3662. [CrossRef] [PubMed]

150. Chu, H.; Liu, Z.; Liang, W.; Zhou, Q.; Zhang, Y.; Lei, K.; Tang, M.; Cao, Y.; Chen, S.; Peng, S.; et al. Radiomics using CT images for preoperative prediction of futile resection in intrahepatic cholangiocarcinoma. *Eur. Radiol.* **2021**, *31*, 2368–2376. [CrossRef]

151. Granata, V.; Fusco, R.; De Muzio, F.; Cutolo, C.; Setola, S.V.; Grassi, R.; Grassi, F.; Ottaiano, A.; Nasti, G.; Tatangelo, F.; et al. Radiomics textural features by MR imaging to assess clinical outcomes following liver resection in colorectal liver metastases. *Radiol. Med.* **2022**, *127*, 461–470. [CrossRef]

152. Zhang, S.; Huang, S.; He, W.; Wei, J.; Huo, L.; Jia, N.; Lin, J.; Tang, Z.; Yuan, Y.; Tian, J.; et al. Radiomics-Based Preoperative Prediction of Lymph Node Metastasis in Intrahepatic Cholangiocarcinoma Using Contrast-Enhanced Computed Tomography. *Ann. Surg. Oncol.* **2022**, *29*, 6786–6799. [CrossRef]

153. Xiang, F.; Wei, S.; Liu, X.; Liang, X.; Yang, L.; Yan, S. Radiomics Analysis of Contrast-Enhanced CT for the Preoperative Prediction of Microvascular Invasion in Mass-Forming Intrahepatic Cholangiocarcinoma. *Front. Oncol.* **2021**, *11*, 774117. [CrossRef] [PubMed]

154. Zhu, Y.; Chen, J.; Kong, W.; Mao, L.; Kong, W.; Zhou, Q.; Zhou, Z.; Zhu, B.; Wang, Z.; He, J.; et al. Predicting idh mutation status of intrahepatic cholangiocarcinomas based on contrast-enhanced CT features. *Eur. Radiol.* **2018**, *28*, 159–169. [CrossRef] [PubMed]

155. Zhu, Y.; Mao, Y.; Chen, J.; Qiu, Y.; Guan, Y.; Wang, Z.; He, J. Value of contrast-enhanced CT texture analysis in predicting IDH mutation status of intrahepatic cholangiocarcinoma. *Sci. Rep.* **2021**, *11*, 6933. [CrossRef]

156. Zhang, Y.; Esmail, A.; Mazzaferro, V.; Abdelrahim, M. Newest Therapies for Cholangiocarcinoma: An Updated Overview of Approved Treatments with Transplant Oncology Vision. *Cancers* **2022**, *14*, 5074. [CrossRef]

157. Gruttadauria, S.; Barbara, M.; Liotta, R. Liver transplantation for unresectable intrahepatic cholangiocarcinoma: An Italian experience. *Updates Surg.* **2021**, *73*, 1587–1588. [CrossRef] [PubMed]

158. Halder, R.; Amaraneni, A.; Shroff, R.T. Cholangiocarcinoma: A review of the literature and future directions in therapy. *Hepatobiliary Surg. Nutr.* **2022**, *11*, 555–566. [CrossRef]

159. Tsilimigras, D.I.; Sahara, K.; Wu, L.; Moris, D.; Bagante, F.; Guglielmi, A.; Aldrighetti, L.; Weiss, M.; Bauer, T.W.; Alexandrescu, S.; et al. Very Early Recurrence After Liver Resection for Intrahepatic Cholangiocarcinoma: Considering Alternative Treatment Approaches. *JAMA Surg.* **2020**, *155*, 823–831. [CrossRef]

160. Loffredo, D.; Marvaso, A.; Ceraso, S.; Cinelli, N.; Rocca, A.; Vitale, M.; Rossi, M.; Genovese, E.; Amato, B.; Cinelli, M. Minimal invasive surgery in treatment of liver metastases from colorectal carcinomas: Case studies and survival rates. *BMC Surg.* **2013**, *13* (Suppl. S2), S45. [CrossRef]

161. Bartolini, I.; Risaliti, M.; Fortuna, L.; Agostini, C.; Ringressi, M.N.; Taddei, A.; Muiesan, P. Current management of intrahepatic cholangiocarcinoma: From resection to palliative treatments. *Radiol. Oncol.* **2020**, *54*, 263–271. [CrossRef]

162. Masci, G.M.; Ciccarelli, F.; Mattei, F.I.; Grasso, D.; Accarpio, F.; Catalano, C.; Laghi, A.; Sammartino, P.; Iafrate, F. Role of CT texture analysis for predicting peritoneal metastases in patients with gastric cancer. *Radiol. Med.* **2022**, *127*, 251–258. [CrossRef]

163. Rocca, A.; Scacchi, A.; Cappuccio, M.; Avella, P.; Bugiantella, W.; De Rosa, M.; Costa, G.; Polistena, A.; Codacci-Pisanelli, M.; Amato, B.; et al. Robotic surgery for colorectal liver metastases resection: A systematic review. *Int. J. Med. Robot.* **2021**, *17*, e2330. [CrossRef] [PubMed]

164. Sijberden, J.P.; Cipriani, F.; Lanari, J.; Russolillo, N.; Benedetti Cacciaguerra, A.; Osei-Bordom, D.; Conci, S.; Görgec, B.; Primrose, J.N.; Edwin, B.; et al. Minimally invasive ver-sus open liver resection for hepatocellular carcinoma in the elderly: International multicentre propensity score-matched study. *Br. J. Surg.* **2022**, *13*, znac423. [CrossRef] [PubMed]

165. Rocca, A.; Cipriani, F.; Belli, G.; Berti, S.; Boggi, U.; Bottino, V.; Cillo, U.; Cescon, M.; Cimino, M.; Corcione, F.; et al. The Italian Consensus on minimally invasive simultaneous resections for synchronous liver metastasis and primary colorectal cancer: A Delphi methodology. *Updates Surg.* **2021**, *73*, 1247–1265. [CrossRef]

166. Arizza, G.; Russolillo, N.; Ferrero, A.; Syn, N.L.; Cipriani, F.; Aghayan, D.; Marino, M.V.; Memeo, R.; Mazzaferro, V.; Chiow, A.K.H.; et al. Impact of tumor size on the difficulty of laparoscopic left lateral sectionectomies. *J. Hepatobiliary Pancreat. Sci.* **2022**; *early view*. [CrossRef]

167. Ceccarelli, G.; Rocca, A.; De Rosa, M.; Fontani, A.; Ermili, F.; Andolfi, E.; Bugiantella, W.; Levi Sandri, G.B. Minimally invasive robotic-assisted combined colorectal and liver excision surgery: Feasibility, safety and surgical technique in a pilot series. *Updates Surg.* **2021**, *73*, 1015–1022, Erratum in *Updates Surg* **2021**, *73*, 1023–1027. [CrossRef]

168. Magistri, P.; Assirati, G.; Ballarin, R.; Di Sandro, S.; Di Benedetto, F. Major robotic hepatectomies: Technical considerations. *Updates Surg.* **2021**, *73*, 989–997. [CrossRef]

169. Zhao, Z.; Yin, Z.; Pan, L.; Li, C.; Hu, M.; Lau, W.Y.; Liu, R. Robotic hepatic resection in postero-superior region of liver. *Updates Surg.* **2021**, *73*, 1007–1014. [CrossRef]

170. Calise, F.; Giuliani, A.; Sodano, L.; Crolla, E.; Bianco, P.; Rocca, A.; Ceriello, A. Segmentectomy: Is minimally invasive surgery going to change a liver dogma? *Updates Surg.* **2015**, *67*, 111–115. [CrossRef] [PubMed]

171. Lendoire, J.C.; Gil, L.; Imventarza, O. Intrahepatic cholangiocarcinoma surgery: The impact of lymphadenectomy. *Chin. Clin. Oncol.* **2018**, *7*, 53. [CrossRef]

172. Kanno, H.; Hisaka, T.; Fujiyoshi, K.; Akiba, J.; Hashimoto, K.; Fujita, F.; Akagi, Y. Prognostic Significance of the Histopathological Growth Pattern and Tumor-Infiltrating Lymphocytes in Stratifying Survival After Hepatectomy for Colorectal Liver Metastases. *Ann. Surg. Oncol.* **2022**, *30*, 3139–3147. [CrossRef] [PubMed]

173. Sutton, T.L.; Wong, L.H.; Walker, B.S.; Dewey, E.N.; Eil, R.; Lopez, C.D.; Kardosh, A.; Chen, E.Y.; Rocha, F.G.; Billingsley, K.G.; et al. Hepatectomy is associated with improved oncologic outcomes in recurrent colorectal liver metastases: A propensity-matched analysis. *Surgery*, 2022; *in press*. [CrossRef] [PubMed]

174. Shen, W.F.; Zhong, W.; Xu, F.; Kan, T.; Geng, L.; Xie, F.; Sui, C.J.; Yang, J.M. Clinicopathological and prognostic analysis of 429 patients with intrahepatic cholangiocarcinoma. *World J. Gastroenterol.* **2009**, *15*, 5976–5982. [CrossRef]

175. Zhang, D.; Zeng, H.; Pan, Y.; Zhao, Y.; Wang, X.; Chen, J.; Wang, J.; Zhang, Y.; Zhou, Z.; Xu, L.; et al. Liver Tumor Markers, HALP Score, and NLR: Simple, Cost-Effective, Easily Accessible Indexes for Predicting Prognosis in ICC Patients after Surgery. *J. Pers. Med.* **2022**, *12*, 2041. [CrossRef] [PubMed]

176. Viganò, L.; Galvanin, J.; Cimino, M.; Torzilli, G. Laparoscopic application of the hooking technique for ultrasound-guided minimally invasive liver surgery. *Updates Surg.* **2022**, *74*, 373–377. [CrossRef] [PubMed]

177. Li, J.; Cao, B.; Bi, X.; Chen, W.; Wang, L.; Du, Z.; Zhang, X.; Yu, X. Evaluation of liver function in patients with chronic hepatitis B using Gd-EOB-DTPA-enhanced T1 mapping at different acquisition time points: A feasibility study. *Radiol. Med.* **2021**, *126*, 1149–1158. [CrossRef]

178. Hyodo, R.; Takehara, Y.; Naganawa, S. 4D Flow MRI in the portal venous system: Imaging and analysis methods, and clinical applications. *Radiol. Med.* **2022**, *127*, 1181–1198. [CrossRef]

179. Gentile, D.; Donadon, M.; Civilini, E.; Torzilli, G. Total upper transversal hepatectomy with outflow reconstruction for advanced mass-forming cholangiocarcinoma. *Updates Surg.* **2021**, *73*, 769–773. [CrossRef] [PubMed]

180. Ruzzenente, A.; Alaimo, L.; Conci, S.; De Bellis, M.; Marchese, A.; Ciangherotti, A.; Campagnaro, T.; Guglielmi, A. Hyper accuracy three-dimensional (HA3D™) technology for planning complex liver resections: A preliminary single center experience. *Updates Surg.* **2022**, *75*, 105–114. [CrossRef] [PubMed]

181. Zerunian, M.; Pucciarelli, F.; Caruso, D.; Polici, M.; Masci, B.; Guido, G.; De Santis, D.; Polverari, D.; Principessa, D.; Benvenga, A.; et al. Artificial intelligence based image quality enhancement in liver MRI: A quantitative and qualitative evaluation. *Radiol. Med.* **2022**, *127*, 1098–1105. [CrossRef]

182. Sammon, J.; Fischer, S.; Menezes, R.; Hosseini-Nik, H.; Lewis, S.; Taouli, B.; Jhaveri, K. MRI features of combined hepatocellular-cholangiocarcinoma versus mass forming intrahepatic cholangiocarcinoma. *Cancer Imaging* **2018**, *18*, 8. [CrossRef]

183. Bilreiro, C.; Soler, J.C.; Ayuso, J.R.; Caseiro-Alves, F.; Ayuso, C. Diagnostic value of morphological enhancement patterns in the hepatobiliary phase of gadoxetic acid-enhanced MRI to distinguish focal nodular hyperplasia from hepatocellular adenoma. *Radiol. Med.* **2021**, *126*, 1379–1387. [CrossRef]

184. Jhaveri, K.S.; Hosseini-Nik, H. MRI of cholangiocarcinoma. *J. Magn. Reson. Imaging* **2015**, *42*, 1165–1179. [CrossRef] [PubMed]

185. Kwon, S.; Kim, Y.K.; Park, H.J.; Jeong, W.K.; Lee, W.J.; Choi, D. Is gadoxetic acid-enhanced MRI limited in tumor characterization for patients with chronic liver disease? *Magn. Reson. Imaging* **2014**, *32*, 1214–1222. [CrossRef] [PubMed]

186. Hamm, C.A.; Wang, C.J.; Savic, L.J.; Ferrante, M.; Schobert, I.; Schlachter, T.; Lin, M.; Duncan, J.S.; Weinreb, J.C.; Chapiro, J.; et al. Deep learning for liver tumor diagnosis part I: Development of a convolutional neural network classifier for multi-phasic MRI. *Eur. Radiol.* **2019**, *29*, 3338–3347. [CrossRef] [PubMed]

187. Wang, C.J.; Hamm, C.A.; Savic, L.J.; Ferrante, M.; Schobert, I.; Schlachter, T.; Lin, M.; Weinreb, J.C.; Duncan, J.S.; Chapiro, J.; et al. Deep learning for liver tumor diagnosis part II: Convolutional neural network interpretation using radiologic imaging features. *Eur. Radiol.* **2019**, *29*, 3348–3357. [CrossRef]

188. Zhou, Y.; Zhou, G.; Zhang, J.; Xu, C.; Wang, X.; Xu, P. Radiomics signature on dynamic contrast-enhanced MR images: A potential imaging biomarker for prediction of microvascular invasion in mass-forming intrahepatic cholangiocarcinoma. *Eur. Radiol.* **2021**, *31*, 6846–6855. [CrossRef]

189. Huang, F.; Liu, X.; Liu, P.; Xu, D.; Li, Z.; Lin, H.; Xie, A. The Application Value of MRI T2*WI Radiomics Nomogram in Discriminating Hepatocellular Carcinoma from Intrahepatic Cholangiocarcinoma. *Comput. Math. Methods Med.* **2022**, *2022*, 7099476. [CrossRef] [PubMed]

190. Hu, R.; Li, H.; Horng, H.; Thomasian, N.M.; Jiao, Z.; Zhu, C.; Zou, B.; Bai, H.X. Automated machine learning for differentiation of hepatocellular carcinoma from intrahepatic cholangiocarcinoma on multiphasic MRI. *Sci. Rep.* **2022**, *12*, 7924. [CrossRef]

191. Song, W.; Chen, Q.; Guo, D.; Jiang, C. Preoperative estimation of the survival of patients with unresectable hepatocellular carcinoma achieving complete response after conventional transcatheter arterial chemoembolization: Assessments of clinical and LI-RADS MR features. *Radiol. Med.* **2022**, *127*, 939–949. [CrossRef]

192. Xu, L.; Wan, Y.; Luo, C.; Yang, J.; Yang, P.; Chen, F.; Wang, J.; Niu, T. Integrating intratumoral and peritumoral features to predict tumor recurrence in intrahepatic cholangiocarcinoma. *Phys. Med. Biol.* **2021**, *66*, 125001. [CrossRef]

193. Zhao, L.; Ma, X.; Liang, M.; Li, D.; Ma, P.; Wang, S.; Wu, Z.; Zhao, X. Prediction for early recurrence of intrahepatic mass-forming cholangiocarcinoma: Quantitative magnetic resonance imaging combined with prognostic immunohistochemical markers. *Cancer Imaging* **2019**, *19*, 49. [CrossRef]

194. Xu, L.; Yang, P.; Liang, W.; Liu, W.; Wang, W.; Luo, C.; Wang, J.; Peng, Z.; Xing, L.; Huang, M.; et al. A radiomics approach based on support vector machine using MR images for preoperative lymph node status evaluation in intrahepatic cholangiocarcinoma. *Theranostics* **2019**, *9*, 5374–5385. [CrossRef]

195. Nishioka, E.; Tsurusaki, M.; Kozuki, R.; Im, S.W.; Kono, A.; Kitajima, K.; Murakami, T.; Ishii, K. Comparison of Conventional Imaging and 18F-Fluorodeoxyglucose Positron Emission Tomography/Computed Tomography in the Diagnostic Accuracy of Staging in Patients with Intrahepatic Cholangiocarcinoma. *Diagnostics* **2022**, *12*, 2889. [CrossRef]

196. Cellina, M.; Gibelli, D.; Martinenghi, C.; Giardini, D.; Soresina, M.; Menozzi, A.; Oliva, G.; Carrafiello, G. Non-contrast magnetic resonance lymphography (NCMRL) in cancer-related secondary lymphedema: Acquisition technique and imaging findings. *Radiol. Med.* **2021**, *126*, 1477–1486. [CrossRef] [PubMed]

197. Zhang, J.; Wu, Z.; Zhang, X.; Liu, S.; Zhao, J.; Yuan, F.; Shi, Y.; Song, B. Machine learning: An approach to preoperatively predict PD-1/PD-L1 expression and outcome in intrahepatic cholangiocarcinoma using MRI biomarkers. *ESMO Open* **2020**, *5*, e000910. [CrossRef] [PubMed]

198. Zhou, Y.; Zhou, G.; Zhang, J.; Xu, C.; Zhu, F.; Xu, P. DCE-MRI based radiomics nomogram for preoperatively differentiating combined hepatocellular-cholangiocarcinoma from mass-forming intrahepatic cholangiocarcinoma. *Eur. Radiol.* **2022**, *32*, 5004–5015. [CrossRef] [PubMed]

199. Qian, X.; Lu, X.; Ma, X.; Zhang, Y.; Zhou, C.; Wang, F.; Shi, Y.; Zeng, M. A Multi-Parametric Radiomics Nomogram for Preoperative Prediction of Microvascular Invasion Status in Intrahepatic Cholangiocarcinoma. *Front. Oncol.* **2022**, *12*, 838701. [CrossRef] [PubMed]

200. Soyer, P.; Fishman, E.K.; Rowe, S.P.; Patlas, M.N.; Chassagnon, G. Does artificial intelligence surpass the radiologist? *Diagn. Interv. Imaging* **2022**, *103*, 445–447. [CrossRef]